Advances in Engineering Software 193 (2024) 103651

Contents lists available at ScienceDirect

Advances in Engineering Software

journal homepage: www.elsevier.com/locate/advengsoft

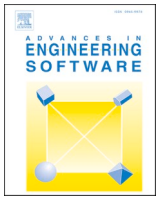

Review

Modelling electro-mechanical behaviour in piezoelectric composites: Current status and perspectives on homogenisation

Pedro M. Ferreira [a,*], Miguel A. Machado [a,b], Catarina Vidal [a,b], Marta S. Carvalho [a,b]

[a] UNIDEMI, Department of Mechanical and Industrial Engineering, NOVA School of Science and Technology, Universidade NOVA de Lisboa, 2829-516 Caparica, Portugal
[b] Laboratório Associado de Sistemas Inteligentes, LASI, 4800-058 Guimarães, Portugal

ARTICLE INFO

Keywords:
Piezoelectric composites
Electro-mechanical properties
Analytical models
Numerical models
Finite element models

ABSTRACT

Piezoelectric composites have emerged as a versatile platform with immense potential for tailoring electro-mechanical properties to cater to a wide spectrum of applications. Central to employing their capabilities are modelling and homogenisation techniques, both analytical and numerical, which serve as the cornerstone of analysing and optimising these materials applications. As technology continues to evolve, the development of sophisticated models and innovative composite designs promises to drive further advancements in the realm of piezoelectric composites. This comprehensive review explores the analytical and numerical models employed for homogenising piezoelectric composites. It systematically presents and scrutinises these models, shedding light on their distinct advantages and limitations, thereby aiding researchers in selecting the most appropriate one for their specific needs. This review highlights challenges in modelling long-fibre composites, citing limitations in Eshelby-Type Models. Simplifying micromechanics-based models encounters challenges when dealing with transverse properties, while Asymptotic Homogenization-Based Models excel in regular patterns. Limited experimental validation exists, particularly in metallic matrices. In conclusion, this comprehensive review navigates the diverse landscape of modelling strategies for Representative Volume Elements, each with its unique strengths and limitations. Researchers in this field must judiciously select modelling techniques based on their piezoelectric characteristics and desired accuracy levels. Additionally, the pressing need for further experimental validation, especially concerning metallic matrices, stands out as a critical avenue for enhancing the reliability and real-world applicability of these modelling techniques.

1. Introduction

Piezoelectric composites represent a fascinating field of research and development in materials science and engineering. These materials offer unique electro-mechanical properties that have found diverse applications in various industries, including sensors, actuators, and energy harvesting devices [1–3]. In this review, it will be possible to prospect into the modelling and homogenisation techniques employed to understand and harness the electro-mechanical properties of piezoelectric composites.

Piezoelectric materials generate an electrical charge when subjected to mechanical stress and, conversely, deform in response to an applied electric field. These properties have been extensively exploited in numerous applications, but the development of piezoelectric composites takes the concept a step further. By combining piezoelectric materials with other materials, such as polymers [4–9], ceramics [10,11], or metals [12–18], engineers can design composites with tailored properties that outperform individual components. Piezoelectric materials, known for their distinctive ability to convert mechanical energy into electrical energy and vice versa, have been the focus of extensive research for many decades. The limitations associated with traditional monolithic piezoelectric materials, such as environmental concerns regarding lead-based systems and brittleness, have driven recent investigations into alternative piezoelectric materials and composite piezoelectric materials [19]. It has been demonstrated that the composite approach, which involves either adding different phases to create two-phase composites or creating porous piezoelectric materials through subtractive methods, can be effectively employed to customise the overall mechanical, piezoelectric, and dielectric properties of these materials [20].

* Corresponding author.
E-mail address: pdm.ferreira@campus.fct.unl.pt (P.M. Ferreira).

https://doi.org/10.1016/j.advengsoft.2024.103651
Received 9 January 2024; Received in revised form 30 March 2024; Accepted 19 April 2024
Available online 9 May 2024

One notable application of piezoelectric composites is in energy harvesting, where these materials can convert mechanical vibrations into electrical energy. The analysis and further identification of the electro-mechanical properties of composites is critical in designing efficient energy harvesting devices for applications ranging from wearable electronics to structural health monitoring systems [21–23]. Moreover, piezoelectric composites find use in sensor technologies, particularly in the development of ultrasonic sensors and transducers for medical imaging, non-destructive testing, and underwater applications [24–31]. Accurate modelling of these composites is vital for optimising sensor performance and ensuring reliability.

To effectively model the electro-mechanical behaviour of these composites, it is crucial to consider the complex interactions between the constituent materials. Homogenisation is a key concept in this context, aiming to describe the overall behaviour of the composite material by analysing the properties and response of its microstructures, as depicted by Guedes and Kikushi [32]. Homogenisation techniques vary in complexity and application, with some focusing on analytical approaches and others relying on numerical simulations [33]. One common analytical approach is the Mori-Tanaka method, which treats the composite as a collection of ellipsoidal or spherical inclusions embedded in a matrix. This method can provide useful insights into the effective properties of the composite but may have limitations when dealing with highly anisotropic behaviour or complex geometries, as it will be possible to see through this review.

Numerical methods, such as the Finite Element Method (FEM), have gained popularity in recent years for modelling piezoelectric composites. FEM allows for the consideration of intricate geometries and material distributions, making it suitable for simulating the electro-mechanical behaviour of complex composite structures. The modelling of piezoelectric composites extends beyond mechanical and electrical aspects since FEM can account for the piezoelectric coupling within the material, providing a more comprehensive understanding of its behaviour.

Thus, piezoelectric composites offer a versatile platform for tailoring electro-mechanical properties to suit a wide range of applications. Modelling and homogenisation techniques, whether analytical or numerical, play a central role in understanding and harnessing the capabilities of these materials. As technology continues to advance, the development of more sophisticated models and innovative composite designs will likely drive further progress in the field of piezoelectric composites. This comprehensive review will present and discuss analytical and numerical models used for homogenising piezoelectric composites. It will highlight the advantages and limitations of each model and draw key conclusions to assist in selecting the most suitable one. Furthermore, it is important to note that the equations considered adhere to the notations adopted in the IEEE Standard on Piezoelectricity, ensuring consistency [34].

2. Electro-mechanical behaviour

Coupled piezoelectric phenomena involve the intricate interplay between electric potential gradients and material deformations. In the indirect piezoelectric effect, the presence of an electric potential gradient induces mechanical deformation, while in the direct piezoelectric effect, mechanical strains give rise to an electric potential gradient. This interconnection between mechanical and electric fields is encapsulated by piezoelectric coefficients. Materials that exhibit linear responses to alterations in electric fields, electric displacements, mechanical stresses, and strains, such as piezoelectric ceramics, polymers, and composites, adhere to these underlying principles. The behaviour of piezoelectric materials can be described by piezoelectric constitutive equations, which establish relationships between stresses (T_{ij}) [Pa], strains (S_{ij}), electric fields (E_k) [N/C or V/m], and electrical displacements (D_i) [C/m^2]. The intrinsic dipole present in the crystalline structure of the material prompts deformation when subjected to an electric field or generates an electrical displacement when mechanically deformed. Nevertheless, these microscopic mechanical deformations or changes in the electric dipole configuration do not inherently translate to evident macroscopic effects. This is due to the fact that these dipoles within the material organise themselves into domains, which exhibit a random distribution within the polycrystalline structure. To observe macroscopic manifestations, these domains need a preferential alignment, a phenomenon referred to as polarisation. The existence of this dipole within the material is responsible for the crystalline structure's deformation under the influence of an electric field and for generating an electrical displacement when mechanically deformed. However, these local mechanical deformations or alterations in electric dipoles are not sufficient to produce significant macroscopic effects, as the dipoles tend to aggregate within domains, which, as previously mentioned, are randomly dispersed within the polycrystalline matrix. To achieve observable macroscopic outcomes, these domains must accomplish a preferred orientation through the process of polarisation [35]. The electrical displacement (D_i) can be expressed as a function of the electric field vector (E_k), the dielectric constants (ε^S_{ik}) [F/m or C/V.m], as well as the mechanical stresses applied to the piezoelectric material (T_{ij}), which is, in turn, dependent on the mechanical deformation (S_{kl}) and the elastic constants (C^E_{ijkl}) [N/m^2 or Pa], as presented in Eq. (1).

$$\begin{cases} T_{ij} = C^E_{ijkl} S_{kl} \\ D_i = \varepsilon^S_{ik} E_k \end{cases} \tag{1}$$

Piezoelectric materials exhibit a compelling interplay between mechanical and electrical factors. Strain, which represents material deformation, is influenced by both mechanical stresses and electric fields. Similarly, electrical displacement is affected by both the applied electric field and mechanical deformation. This coupling phenomenon is encapsulated within Eq. (2), where the piezoelectric tensor d [C/N] is presented, and the superscript T suggests a transposed matrix.

Within Eq. (2), there emerges a fourth-order elasticity tensor (C^E_{ijkl}) under conditions where short circuit boundaries are maintained. Additionally, a second-order electric tensor representing free body conditions (ε^S_{ik}) and a third-order piezoelectric stress tensor (d_{kij}) are observed. Given the symmetry inherent in the tensors T_{ij}, S_{ij}, C^E_{ijkl} and ε^S_{ij}, it becomes feasible to express Eq. (2) using a matrix-based notation, as shown in Eq. (3).

$$\begin{cases} T_{ij} = C^E_{ijkl} S_{kl} - d_{kij} E_k \\ D_i = d_{ikl} S_{kl} + \varepsilon^s_{ik} E_k \end{cases} \tag{2}$$

$$\begin{bmatrix} T \\ D \end{bmatrix} = \begin{bmatrix} C^E & -d^T \\ d & \varepsilon^S \end{bmatrix} \begin{bmatrix} S \\ E \end{bmatrix} \tag{3}$$

When dealing with a piezocomposite material, if the wavelength of the electric field applied to it is much larger than the size of its individual unit cell or microstructure, it is possible to treat the composite as a uniform material. This simplification allows us to describe its behaviour using the already mentioned Eq. (2) and (3), by plugging in the effective properties of the composite, which are also referred to as homogenised properties (see [36]).

To determine these effective properties, a set of models, explained in Section 3 and 4, can be used. As a result of this process, the equations that define how the composite material behaves, now accounting for these homogenised properties, can be expressed in the following Eq. (4). The matrix $[\bar{K}]$ is presented in Eq. (5), where "$\bar{\cdot}$" denotes the homogenised quantities, the subscript "eff" refers to the homogenised properties, C^E_{eff} is the effective compliance tensor under short circuit conditions, ε^S_{eff} is the effective clamped body dielectric tensor, and d_{eff} is the effective piezoelectric stress tensor. The matrix $[\bar{K}]$ presented in Eq. (5) is a 9 × 9 matrix that comprises several components. These components consist of the elastic tensor (C^E_{eff}), a 6 × 6 matrix that represents

material properties under a consistent electrical field. Also included is the piezoelectric tensor (d_{eff}), 3 × 6, along with its transpose (d^{T}_{eff}), forming a 6 × 3 matrix. These components define the connection between mechanical stress and electrical effects. Completing the matrix $[\bar{K}]$ is the dielectric tensor (ε^{S}_{eff}), which is a 3 × 3 matrix.

$$\begin{bmatrix} \bar{T} \\ \bar{D} \end{bmatrix} = [\bar{K}] \begin{bmatrix} \bar{S} \\ \bar{E} \end{bmatrix} \tag{4}$$

$$[\bar{K}] = \begin{pmatrix} C^{E}_{eff} & -d^{T}_{eff} \\ d_{eff} & \varepsilon^{S}_{eff} \end{pmatrix} \tag{5}$$

By understanding and manipulating these components within the matrix $[\bar{K}]$, researchers and engineers can gain profound insights into the behaviour of piezoelectric composite materials, unlocking their potential for applications across a spectrum of industries. This comprehensive approach, encompassing the interaction of electrical and mechanical, material properties, holds promise for driving technological advancements and innovations in various domains.

In the pursuit of further knowledge and progress, it is important to continue exploring these relationships, refining the homogenisation methods, and harnessing the intricate symphony of properties exhibited by piezoelectric composites.

3. Analytical models

Analytical modelling has played a crucial role in understanding the characteristics of various piezoelectric composite materials. Several approaches have been developed to predict the properties of these composites, including the simple mechanics/micromechanics models, Eshelby-type models for ellipsoidal inclusions in a piezoelectric matrix, and the asymptotic homogenization-based models (AHM) for periodic composites.

3.1. Micromechanics-based models

The earliest micromechanics-based models focused on the series-parallel type formulation, first introduced by Hashimoto et al. [37] in 1986 and further developed by Banno et al. [38] in 1987. This formulation provided a good approximation for the electromechanical behaviour of piezoelectric composites with the type of connectivity designated as 2–2 (Fig. 1a)). However, there are other types of connectivity for piezoelectric composites that take into account the arrangement and distribution of the piezoelectric elements within the matrix material, such as 0–3, 1–3, and 3–3 connectivities. In a 0–3 connectivity, the piezoelectric elements are dispersed randomly in a three-dimensional manner within the matrix material. This random distribution provides isotropic properties, meaning that the composite exhibits similar piezoelectric properties in all directions. 0–3 composites are versatile and can be used in various applications where omnidirectional sensitivity is needed (Fig. 1b)). A 1–3 connectivity involves piezoelectric elements arranged as cylindrical rods or fibres embedded within the matrix material. These rods or fibres run predominantly in one direction (e.g., vertically) while the matrix material surrounds them. This arrangement offers high piezoelectric coefficients in the direction of the rods, making 1–3 composites suitable for applications requiring directional sensitivity or high electromechanical coupling (Fig. 1c)). In a 3–3 connectivity, piezoelectric elements are distributed three-dimensionally, similar to 0–3 composites. However, unlike 0–3 composites, 3–3 composites have better control over the orientation and alignment of the piezoelectric elements. This allows for improved customisation of the material's properties and performance characteristics. 3–3 composites are often used when precise control over the material's behaviour is necessary for specific applications (Fig. 1d)).

Consider a 2–2 piezocomposite, where two different materials are combined in a specific arrangement. These materials are aligned in series, following a particular direction called the poling direction. The equations that describe how these materials respond to electrical and mechanical forces have been compactly expressed by Hashimoto et al. [37] for each phase within the composite. This composite consists of a polymer phase (designated by subscript p) and a ceramic phase (designated by subscript c). The piezoelectric constitutive equations are written in Eqs. (6) and (7), and the homogenised material equation is presented in Eq. (8).

$$(TD)^{c} = [K]^{c}(SE)^{c} \tag{6}$$

$$(TD)^{p} = [K]^{p}(SE)^{p} \tag{7}$$

$$(\overline{TD}) = [\bar{K}](\overline{SE}) \tag{8}$$

Eqs. (6)–(8) involve two vectors, denoted as (TD) and (SE), each consisting of nine components. The vector (TD) written in Eq. (9) encompasses six specific components that form the stress tensor (T), along with an additional three components that constitute the electrical displacement (D). Similarly, the vector (SE) written in Eq. (10) is constructed with components derived from the strain tensor (S) and the electrical field vector (E). The 9 × 9 matrix [K] (Eq. (5)), is formed by combining components that include the elastic tensor (C), which is a 6 × 6 matrix representing material properties under a constant electrical field, and the 3 × 6 piezoelectric tensor (d) that describes the relationship between mechanical stress and electrical effects, and the 3 × 3 dielectric tensor (ε).

$$(TD) = (T_1, T_2, T_3, T_4, T_5, T_6, D_1, D_2, D_3) \tag{9}$$

$$(SE) = (S_1, S_2, S_3, S_4, S_5, S_6, E_1, E_2, E_3) \tag{10}$$

To derive the effective matrix [K] for the 2–2 connectivity configuration, it was established continuity conditions for every individual component of (T), (D), (S), and (E) across the composite. There are 18 conditions in total, and for each of them, can be express the conditions using two distinct approaches: either employing simple series or parallel models.

In the first approach, a component remains constant throughout the composite, such as $S^{c}_{1} = S^{p}_{1} = \overline{S_1}$. Alternatively, the second approach

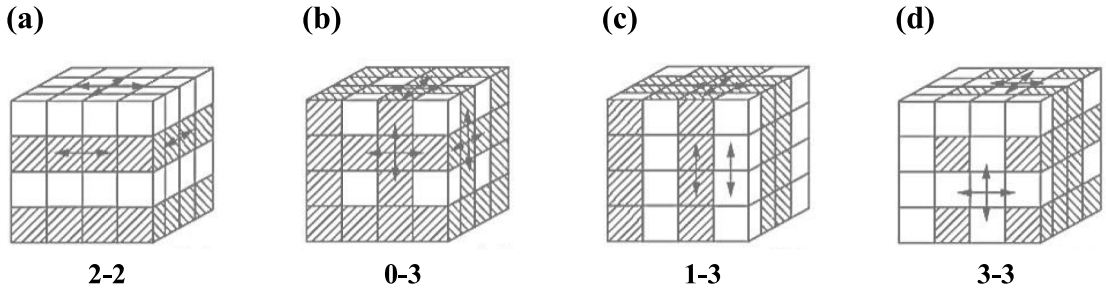

Fig. 1. Different types of connectivity for piezoelectric composites (based on [39]).

involves calculating a weighted sum of the components from each phase, like $\overline{T_1} = \nu T_1^c + (1-\nu)T_1^p$, where ν represents the ceramic's volume fraction.

However, these equations are applicable only when all field quantities within the two phases are uniform, and the interfaces have rigid boundary conditions. This means that stress and electrical displacement perpendicular to the interface, as well as strain and electrical field parallel to the interface, remain continuous.

Within the matrix-based method, assumptions are made regarding isostrain and isostress conditions at the composite surfaces. The vectors (TD) and (SE) consist of components with different characteristics (constant and averaged), which require distinct treatment for subsequent calculations. Hence, it's advantageous to introduce two new vectors: one that comprises entirely constant components (G) and another that encompasses all averaged components (H).

For the 2–2 piezocomposite, vectors (G) and (H) are determined by Eqs. (11) and (12), respectively.

$$(G) = (S_1, S_2, T_3, T_4, T_5,\ S_6, E_1,\ E_2,\ D_3) \tag{11}$$

$$(H) = (T_1, T_2, S_3, S_4, S_5,\ T_6, D_1,\ D_2,\ E_3) \tag{12}$$

The newly established basis (G, H) serves the purpose of representing the vectors (TD) and (SE). Notably, in Eqs. (13) and (14), diagonal matrices denoted as [P] and [Q] are employed, highlighting the structure of the expressions. By utilising the expressions presented in Eqs. (6)–(8), (11) and (12), a straightforward connection between the vectors (H) and (G) becomes apparent. This connection is facilitated through the utilisation of a matrix labeled as [W], as written in Eq. (15).

$$(TD) = [Q](H) - [P](G) \tag{13}$$

$$(SE) = [Q](G) - [P](H) \tag{14}$$

$$(H) = [W](G) \tag{15}$$

Eq. (15) holds true for each of the phases individually, and therefore, it extends its validity to the composite, which is illustrated in Eq. (16).

$$(\bar{H}) = [\bar{W}](\bar{G}) \tag{16}$$

Having a grasp of the matrix [W], subsequent to a series of calculations and manipulations, leads to the derivation of the effective matrix $[\bar{K}]$. This effective matrix is shown in Eq. (17).

$$[\bar{K}] = \{[P] - [Q][\bar{W}]\}\{[P][\bar{W}] - [Q]\}^{-1} \tag{17}$$

An advantageous aspect of this approach lies in the fact that the two vectors, (G) and (H), are solely reliant on the placement of the interfacial planes that demarcate the two phases. This dependence extends specifically to the composite's arrangement. Consequently, this method can be universally employed across different configurations, including the 1–3, 0–3, and 3–3 connectivities (Fig. 1b)–d)), as highlighted in references [40–42].

The work by Kim et al. [43] in this area considered purely elastic multi-layers. Building on this, Levassort et al. [40–42] extended the matrix method of Hashimoto et al. [37] to investigate effective electromechanical properties in 1–3, 0–3, and 3–3 type piezoelectric composites. While these models were somewhat simplistic, they offered reasonable estimates for specific geometric configurations of inclusions within the piezoelectric matrix. Subsequently, Wang et al. [44] and Topolov and Krivoruchko [45] contributed analytical schemes capable of predicting the electromechanical properties of layered piezoelectric materials with varying levels of elastic anisotropy. Additionally, Bowen et al. [46] introduced a model for predicting the behaviour of 0–3 type porous piezoelectric composites and 3–3 type piezoelectric composites. Kar-Gupta et al. [47,48] also made significant contributions in this field. This author developed simple micromechanics models to predict the electromechanical properties of 1–3 type long-fibre piezoelectric composites and extended their work to cover 2–2 type layered composites with anisotropic constituents. Tan et al. [49] employed micro-electromechanical models, specifically the rectangular and rectangle-cylinder models. These models allowed them to derive analytical formulas for predicting various properties like elasticity, piezoelectricity, and dielectric behaviour of fibre-reinforced piezoelectric composites. These predictions were then compared with results obtained from the FEM. There exist multiple micromechanical-based models for estimating the effective properties of piezoelectric composites. For instance, the method of cells and strength of materials approaches [50,51] serve this purpose. Aimmanee et al. [52] utilised such a micromechanical model to ascertain the effective thermo-electro-mechanical characteristics of a composite composed of hollow piezoelectric fibres. The outcomes derived from this model were in agreement with results from FEM analysis. In a similar vein, Singh et al. [53] proposed a micromechanics-based technique to analyse how the arrangement of fibres within the composite impacts its overall properties. They adapted the traditional strength of materials model to investigate the influence of fiber packing on the composite's properties. In their work, the effective material coefficients were evaluated using the finite element method.

However, the results from these studies did not demonstrate an enhancement in the effective values of piezoelectric constants compared to those of bulk piezoelectric materials. This might be attributed to the fact that these models calculated effective coefficients based on the average electric field within the homogenised piezoelectric composite. Yet, practical situations involve significantly lower electric fields within piezoelectric fibres in comparison to the matrix phase, owing to their substantial differences in dielectric properties.

Odegard et al. [54] also carried out a comparative analysis that compared micromechanical predictions of electroelastic properties with finite element analysis results for piezoelectric composites. Additionally, Dinzart et al. [55] recently introduced a novel micromechanical model aimed at assessing the electroelastic behaviour of piezoelectric composites featuring coated reinforcements.

A common assumption underlying the development of all these micromechanical models was their utilisation of averaged representations for the fields (both mechanical and electric) existing within the constituents of the composite. However, real-world scenarios reveal that these values exhibit strong localisation and are extremely sensitive to fluctuations in local fields. Overall, these studies underscore the complexities of predicting the behaviour of piezoelectric composites and highlight the need for more sophisticated models that can capture the intricate interplay between different factors at play within these materials.

3.2. Eshelby-type models

In the realm of modelling using the Eshelby-type approach, early efforts were primarily directed towards the expansion of Eshelby's solution [56] to encompass anisotropic piezoelectric inclusions within the elastic domain [57,58]. However, despite these endeavours, a closed-form resolution for the elements of the Eshelby tensor remained elusive. Consequently, a numerical methodology was employed to solve for these tensor components in the context of an anisotropic system [59]. Numerous researchers have taken steps to extend Eshelby's classical solution, initially formulated for an infinite medium housing a singular ellipsoidal inclusion, to accommodate scenarios involving piezoelectric constituents [60–63]. This approach is often termed the dilute solution, ignores the interactions between the inclusions that occur at finite inclusion volume fractions. In essence, these endeavours delve into the intricacies of integrating piezoelectric considerations into established models, further enriching our understanding of the behaviour of composite materials.

In the context of a piezoelectric inclusion problem, and a situation where there is a specific region Ω in an infinite domain (denoted as R^3).

This region Ω is characterised by having a constant eigenstrain-eigenelectric field, denoted as Z*. This eigenstrain-eigenelectric field are uniform and unchanging throughout the region Ω. It is important to note that this region, depicted in Fig. 2a) is assumed to be stress-free (no external forces affecting it) and electric displacement-free (no accumulation of electric charge at its boundaries). This problem is defined, mathematically, by Eqs. (18)–(20), describe various aspects of the problem [64]:

- U_K represents the displacement for $K = 1,\ 2,\ 3$ and electric potential for $K = 4$.
- Z_{KI} represents the strain for $K = 1,\ 2,\ 3$ and electric field for $K = 4$.
- $\sum iJ$ represents the stress for $J = 1,\ 2,\ 3$ and electric displacement for $J = 4$.
- F_{iJKl} represents the piezoelectric moduli.

$$\sum iJ, i = 0 \tag{18}$$

$$\sum iJ = F_{ijKl}\left[Z_{Kl} - Z^{*}_{Kl}(x)\right] \tag{19}$$

$$F_{iJKl}Z_{Kl} = F_{iJKl}U_{K,l} \tag{20}$$

Central to the problem is the eigenstrain – eigenelectric field $Z^{*}_{Kl}(x)$, which is defined by Eq. (21).

$$Z^{*}_{Kl}(x) = Z^{*}_{Kl}\ x \in \Omega\ 0\ x \in R^3 - \Omega \tag{21}$$

Substituting the Eq. (21) into Eq. (18), it was possible to obtain the Eq. (22).

$$F_{iJKl}U_{K,li} = F_{iJKl}\partial_i Z^{*}_{Kl}(x) \tag{22}$$

The Eq. (22) demonstrates that the quantity represented by $F_{iJKl}\partial_i Z^{*}_{Kl}(x)$ can be interpreted as body force-electric charge density, where ∂_i represents the partial differentiation with respect to x_i. Deeg's work in 1980 [65] derived a comprehensive solution for this particular issue in an integral form. Particularly intriguing is the scenario where the inclusion shape Ω takes the form of an ellipsoid. In this problem, the strain-electric field Z within Ω resulting from Z* can sometimes be explicitly determined by performing an analytical evaluation. Notably, Deeg's dissertation [65] did not carry out this specific analytical assessment. The outcome established by Deeg [65] for the case of ellipsoidal inclusions can be reformulated into the following form (Eq. (23)), where S_{KlAb} is a piezoelectric analog of Eshelby tensor.

$$Z_{Kl} = S_{KlAb}Z^{*}_{Ab} \text{ in } \Omega \tag{23}$$

The expression for S_{KlAb} is provided through Eqs. (24) and (25), where I_{ilKJ} is determined by Eq. (26), and a_i represents the length of the semi-axis of the ellipsoid in the direction of x_i. Given that S_{KlAb} is composed of four distinct tensors, this paper refers to it as the piezoelectric Eshelby tensors, as also mentioned in Mikata et al. [64]. The condition $|x| = 1$ corresponds to the surface of a unit sphere, and H^{-1}_{KJ} denotes the inverse of the 4×4 matrix H_{KJ}, which is defined by Eq. (28). The configuration of the ellipsoid's shape influences the piezoelectric Eshelby tensors, denoted as S_{KlAb}, through the parameter μ outlined in Eq. (27), which appears in the integrand. Notably, the coordinate axes are deliberately aligned with the axes of the ellipsoid.

$$S_{KlAb} = 18\pi F_{iJAb}(I_{ikJ} + I_{ilkJ}) \text{ when } K = 1, 2, 3 \tag{24}$$

$$S_{KlAb} = 14\pi F_{iJAb}I_{ik4J} \text{ when } K = 4 \tag{25}$$

$$I_{ilKJ} = a_1 a_2 a_3 \int_{|x|=1} 1\mu^3 x_i x_l H^{-1}_{KJ} DS \tag{26}$$

$$\mu = a_1^2 x_1^2 + a_2^2 x_2^2 + a_3^2 x_3^2 \tag{27}$$

$$H_{KJ} = F_{pKJq}x_p x_q = F_{pJKq}x_p x_q \tag{28}$$

The work initiated by Wang et al. [60] was expanded upon by Martin et al. [66], who furthered the progress in solving the problem of piezoelectric inclusions. An alternative solution approach to this inclusion problem was introduced by Benveniste et al. [61] and Chen [67], building upon the generalised solution from Walpole et al. [58]. Thus, a quartet of tensors that constitute the piezoelectric counterpart of the Eshelby tensor was determined by Dunn et al. [68], Benveniste et al. [61] and Chen [67]. However, they did not provide explicit closed-form expressions for these tensors. In contrast, Dunn et al. [68,69] provided explicit formulations for the equivalent Eshelby tensor, albeit in the context of a surface integral over a unit sphere, necessitating numerical evaluation. Mikata et al. [70], in their investigation specialised for spheroidal inclusions, derived explicit solutions for the Eshelby tensor's components through the resolution of a specific bi-cubic equation outlined in their earlier work [64].

Several other research studies [62,67,68,70–73] have directed their attention towards the classical expansions of Eshelby's solution, which pertain to scenarios involving finite fractions of inclusion volumes. These expansions include methods like the Dilute Approximation, Mori–Tanaka method, Self-consistent method, and Extended Rule of Mixture. Additionally, there have been instances where researchers have derived analytical solutions specific to certain composite systems. Although these various approaches offer a general framework to estimate properties for a broad spectrum of inclusion sizes, shapes, and orientations, each method comes with its limitations in terms of accuracy and computational feasibility. In the sections that follow, it will be possible to see how.

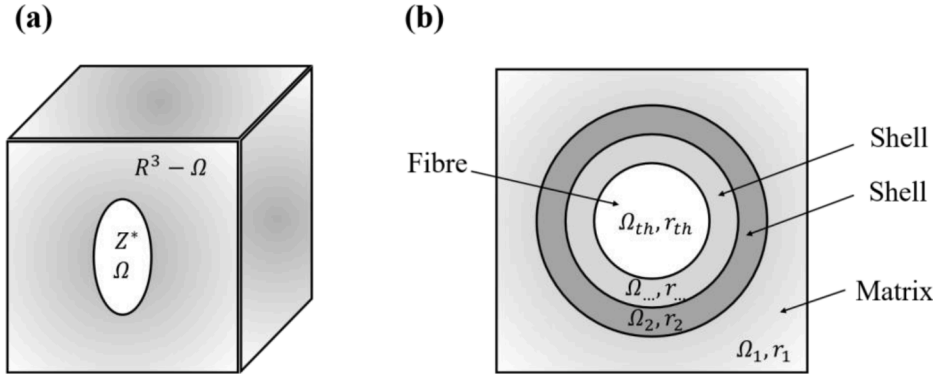

Fig. 2. Eigenstrain – eigenelectric field Z^* in region Ω in an infinite domain R^3 (piezoelectric medium).

3.2.1. Dilute approximation approach

In the context of the Dilute Approximation approach, it assumes that interactions among reinforced particles or fibres within a composite based on a matrix can be neglected. In the case of multiphase composites depicted in Fig. 2b), the concentration tensor associated with each phase r is represented by the Eq. (29). Here, I denotes the 9×9 identity matrix, EE_1 and EE_r stand for the electro-elastic tensor of phase 1 and phase r respectively, and S_r represents the constraint tensor specific to the r_{th} phase. This constraint tensor S_r is an analogous piezoelectric version of Eshelby's tensor, as introduced by Eshelby in 1957 [56]. Essentially, this tensor plays a crucial role in determining the electro-elastic characteristics of a composite material in relation to the inclusion's geometric properties, as discussed in works by Dunn et al. [68]. The detailed expression for the constraint tensor S_r for a fibrous inclusion can be located in other sources, specifically, in Dunn et al. [68] work.

$$A_r^{dil} = \left[I + S_r EE_1^{-1}(EE_r - EE_1)\right]^{-1} \tag{29}$$

3.2.2. Mori-Tanaka approach

The Mori–Tanaka approach, first introduced by Mori and Tanaka in 1973 [74], has found wide application in solving various problems concerning the physical characteristics of composite materials. The fundamental concept underlying the Mori–Tanaka theorem is that the average volume strain around an inclusion, induced by eigenstrains within the inclusion, can be effectively represented without requiring explicit knowledge of the spatial strain distribution (explained further by Dunn et al. [68]).

In the context of the Mori–Tanaka approach, the concentration tensor associated with each phase A_r^{MT} is derived using the concentration tensor A_r^{dil} obtained from the Dilute Approximation approach (Eq. (29)). This relationship is illustrated in Eq. (30), where c_1 and c_r denote the volume fractions of phase 1 and phase r respectively. This process allows the Mori–Tanaka approach to incorporate the effects of inclusion-induced strain interactions while benefiting from the foundation laid by the Dilute Approximation approach.

$$A_r^{MT} = A_r^{dil}\left[c_1 I + \sum_{r=2}^{N} c_r A_r^{dil}\right]^{-1} \tag{30}$$

Malakooti et al. [75] introduced an expanded Mori-Tanka approach coupled with multi-inclusion modelling and finite element simulation. Their approach aimed to predict effective electro-elastic attributes of multiphase piezoelectric composites. Rodríguez-Ramos et al. [76] extended the Maxwell and Mori-Tanaka methodologies to address heterogeneous piezoelectric structures. This allowed them to predict composite effective properties, and they validated their numerical results against several alternative techniques. Hasanzadeh et al. [77] devised a multi-procedure micromechanics strategy rooted in the Mori-Tanaka approach. It was specifically tailored for estimating both elastic and piezoelectric properties. Chen et al. [78] adopted an enhanced Mori-Tanaka homogenisation approach. Their focus was on nanocomposites featuring transversely isotropic piezoelectric phases. A significant aspect of their work involved incorporating the surface piezoelectricity effect. Furthermore, Chen et al. [79] harnessed this effect to derive effective properties of nanoporous piezoelectric materials. Rodriguez-Ramos et al. [80] explored the Maxwell homogenisation technique for assessing the effective electro-elastic attributes of piezoelectric composites. Their study encompassed a comprehensive exploration of varied piezoelectric properties and orientations of inhomogeneities.

3.2.3. Mori–Tanaka approach for multiphase materials

In the context of a complex multiphase composite consisting of N different phases, the comprehensive electroelastic modulus tensor can be described using a multiple inclusion framework, as proposed by Hori et al. [81]. This formulation is outlined in Eq. (31), where A_r^{MT} corresponds to the concentration tensor derived from the Mori–Tanaka approach. This equation enables the representation of the overall electroelastic behaviour by considering the combined effects of various phases and their interactions, utilising the insights provided by the multiple inclusion model.

$$EE = EE_1 + \sum_{r=2}^{N} c_r(EE_r - EE_1)A_r^{MT} \tag{31}$$

3.2.4. Self-Consistent approach

The Self-Consistent approach, initially explored by Hershey [82] and Kröner [83] for analysing linear behaviour in polycrystalline aggregates, involves considering a single heterogeneity (an inclusion) embedded within a uniform medium (matrix). This approach seeks to determine the effective electroelastic moduli, denoted as E_{iJMn}^{eff} for this configuration, while also considering the influence of the surrounding medium on the behaviour of the inclusion.

In contrast to the aforementioned scenario, this model can consider an inclusion embedded in a homogeneous medium with distinct electroelastic moduli, referred to as E_{iJMn}^{I}. Under these conditions, the expression of the field Z^I takes on a particular form. The final formulation of the local field Z^I in terms of the global or macroscopic fields Z_{Kl} is presented through Eqs. (32) or (33). Here, V represents the total volume of the composite medium, encompassing both the inclusion and the matrix.

In these equations, Z_{Kl} corresponds to the macroscopic uniform strain-electric field, and A_{MnKl}^{Sc} is a compact representation for four concentration tensors. This approach allows for the analysis of how the heterogeneity within the composite interacts with its surrounding medium, leading to an understanding of the local field behaviour in relation to the broader composite structure.

$$Z_{Mn}^{I} = I_{KlMn} + 1V^{I}T_{iJKl}^{II}\Delta E_{iJMn}^{I-1}Z_{Kl} \tag{32}$$

$$Z_{Mn}^{I} = A_{MnKl}^{Sc}Z_{Kl} \tag{33}$$

$$\Delta E_{iJMn}^{I} = E_{iJMn}^{I} - E_{iJMn}^{eff} \tag{34}$$

Utilising the previously introduced terminology, the concentration tensor within the framework of the Self-Consistent approach can be reformulated as shown in Eq. (35). In this equation, EE represents the electromechanical moduli of the composite that is yet to be determined. Additionally, the constraint tensor S_r is assessed based on the values of E and a_i^T. This equation's revision provides insight into how the concentration tensor is linked to the composite's electromechanical properties, with the constraint tensor being dependent on both the undetermined moduli EE and the parameter a_i^T.

$$A_r = \left[I + S_r EE^{-1}(EE_r - EE)\right]^{-1} \tag{35}$$

Furthermore, the work by Fakri et al. [71] extended its investigation to derive interaction tensors for the Self-Consistent approach, Mori–Tanaka approach, and Dilute Approximation, aiming to anticipate electroelastic characteristics across diverse reinforcement orientations. The findings of this study indicated that the Mori–Tanaka approach exhibited the highest level of consistency with experimental data, thereby establishing its superior alignment with empirical observations.

3.2.5. Extended rule of mixture approach

The Mori–Tanaka method exhibits limitations when it comes to accurately predicting the effective transverse modulus (where $C_{11}^{eff} = C_{22}^{eff}$) due to its focus solely on volume fraction. As a solution to this, the Extended Rule of Mixture, proposed by Jacquet et al. [84], offers a way to estimate the effective transverse modulus of piezoelectric structural fibre composites by accounting for the size effects of each phase.

For materials consisting of two phases, the Extended Rule of Mixture

provides a means to predict both the longitudinal and transverse moduli of the composite. This approach is captured in Eq. (36), where terms like C_{11}^{eff}, C_{11}^{f}, C_{11}^{m}, and c_f signify the effective composite transverse modulus, the transverse modulus of the fibre reinforcement, the transverse modulus of the matrix, and the volume fraction of the fibre reinforcement, respectively. This equation enables a more comprehensive prediction of the composite's mechanical behaviour, particularly its transverse modulus, by considering the interplay between phases and their size-related effects.

$$C_{11}^{eff} = \frac{C_{11}^{f} C_{11}^{m}}{C_{11}^{m} + C_{11}^{f}\left(1-\sqrt{C_f}\right)/\sqrt{C_f}} + \left(1-\sqrt{C_f}\right) C_{11}^{m} \tag{36}$$

3.3. Asymptotic homogenization-based models

The homogenisation method is a powerful technique applied to complex periodic materials. Particularly in the context of piezoelectricity, the homogenisation allows to calculate the effective properties of these materials by approximating them as a periodic repetition of a unit cell. The method has been extensively discussed in various research papers, such as in Galka et al. [85], Sigmund et al. [86], and Silva et al. [36]. The numerical implementation of this method can be found in the work of Guedes et al. [32], specifically for elasticity problems. In particular, the asymptotic homogenisation, also known as periodic homogenisation, presents an effective and efficient approach to determine the overall mechanical response of composite materials. This method considers that the composite material can be approximated by a periodic repetition of a unit cells. The unit cell is a small domain within the material's microstructure that captures the essential features and geometrical arrangement of the constituents. The central idea of asymptotic homogenisation lies in exploiting the small-scale variations in the microstructure, which occur at a much smaller length scale than the overall dimensions of the composite material. By employing this technique, one can significantly reduce the computational effort needed to obtain the effective properties of the composite. A schematic of homogenisation method approach for periodic microstructure is presented in Fig. 3.

To compute the effective properties, the homogenisation method involves solving auxiliary problems within the unit cell. These auxiliary problems help determine the characteristic displacement (χ), characteristic electrical potential (R), and characteristic coupled functions (Φ and ψ), as described in Silva et al. [36]. The homogenization process takes place within suitable functional spaces, denoted as H_{per} (Y,R^3) and H_{per} (Y), with Y representing the volume of the unit cell. These problems can be formulated in a weak form, which allows for efficient numerical solution, as shown in Eqs. (37)–(40).

$$\int_Y \left[C_{ijkl}^{E}\left(\delta_{im}\delta_{jn} + \frac{\partial \chi_i^{mn}}{\partial y_j}\right) + d_{ikl}\frac{\partial \psi^{mn}}{\partial y_i}\right] S_{kl}(v)\,dY = 0,\ \forall v \in H_{per}\left(Y,\ R^3\right) \tag{37}$$

$$\int_Y \left[d_{kij}\left(\delta_{im}\delta_{jn} + \frac{\partial \chi_i^{mn}}{\partial y_j}\right) - \varepsilon_{ik}^{S}\frac{\partial \psi^{mn}}{\partial y_i}\right] \frac{\partial \varphi}{\partial y_k}\,dY = 0,\ \forall \varphi \in H_{per}(Y) \tag{38}$$

$$\int_Y \left[C_{klij}^{E}\frac{\partial \Phi_k^{m}}{\partial y_l} + d_{kij}\left(\delta_{mk} + \frac{\partial R^{m}}{\partial y_k}\right)\right] S_{ij}(v)\,dY = 0,\ \forall v \in H_{per}\left(Y,\ R^3\right) \tag{39}$$

$$\int_Y \left[d_{kij}\frac{\partial \Phi_i^{m}}{\partial y_j} - \varepsilon_{ik}^{S}\left(\delta_{mi} + \frac{\partial R^{m}}{\partial y_i}\right)\right] \frac{\partial \varphi}{\partial y_k}\,dY = 0,\ \forall \varphi \in H_{per}(Y) \tag{40}$$

Finally, the homogenised properties are obtained through Eqs. (41)–(43). The Kronecker delta symbol (δ_{ip}) is used, and the material property tensors are symmetric to preserve physical symmetries, such as $C_{ijkl}^{H} = C_{ijlk}^{H} = C_{jikl}^{H} = C_{klij}^{H}$, $d_{ijk}^{H} = d_{ikj}^{H}$ and $\varepsilon_{ij}^{H} = \varepsilon_{ji}^{H}$, where "H" represents the homogenised properties.

$$C_{rspq}^{H} = \frac{1}{|Y|}\int_Y \left[C_{ijkl}^{E}\left(\delta_{ip}\delta_{jq} + \frac{\partial \chi_i^{pq}}{\partial y_j}\right)\left(\delta_{kr}\delta_{ls} + \frac{\partial \chi_k^{rs}}{\partial y_l}\right) + d_{kij}\left(\delta_{ip}\delta_{jq} + \frac{\partial \chi_i^{pq}}{\partial y_j}\right)\frac{\partial \psi^{rs}}{\partial y_k}\right] dY \tag{41}$$

$$d_{prs}^{H} = \frac{1}{|Y|}\int_Y \left[d_{kij}\left(\delta_{kp} + \frac{\partial R^{p}}{\partial y_k}\right)\left(\delta_{ir}\delta_{js} + \frac{\partial \chi_i^{rs}}{\partial y_j}\right) - d_{kij}\frac{\partial \Phi_i^{p}}{\partial y_j}\frac{\partial \psi^{rs}}{\partial y_k}\right] dY \tag{42}$$

$$\varepsilon_{pq}^{H} = \frac{1}{|Y|}\int_Y \left[\varepsilon_{ij}^{S}\left(\delta_{ip} + \frac{\partial R^{p}}{\partial y_i}\right)\left(\delta_{jq} + \frac{\partial R^{q}}{\partial y_j}\right) - d_{kij}\left(\delta_{kp} + \frac{\partial R^{p}}{\partial y_k}\right)\frac{\partial \Phi_i^{q}}{\partial y_j}\right] dY \tag{43}$$

In summary, the homogenisation method in the context of piezoelectricity enables to efficiently compute the effective properties of complex periodic materials by considering a representative volume element and solving auxiliary problems. The method's mathematical formulation is done in suitable functional spaces, and the final results preserve the symmetry of material property tensors. This approach is widely used in various research fields, and its numerical implementation allows for accurate and computationally feasible calculations of effective material properties.

The homogenisation method considers the material as a periodic repetition of a unit cell, a small domain that captures the essential microstructural features while maintaining computational efficiency. So, the first step in asymptotic homogenisation is to carefully select an

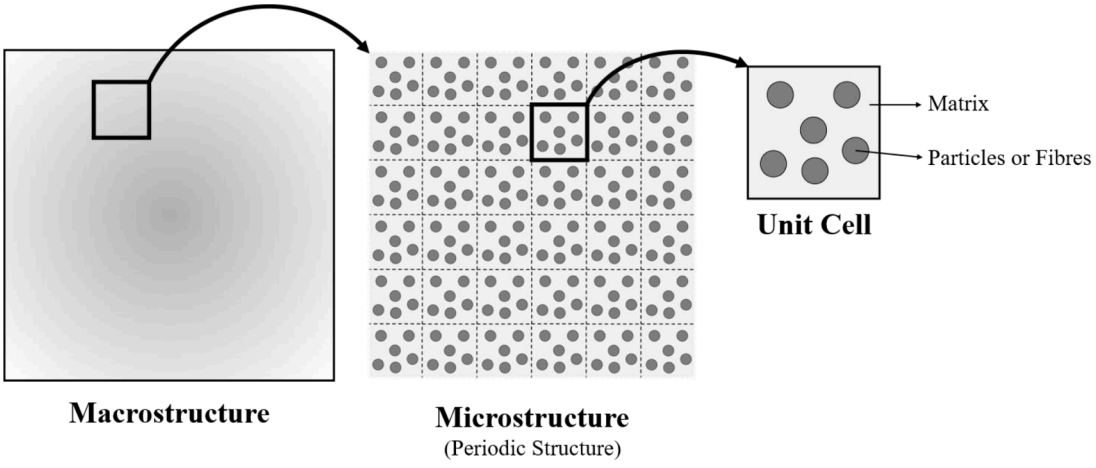

Fig. 3. Schematic of homogenisation method approach for periodic composite materials with periodic microstructure.

appropriate unit cell that is representative of the entire material's microstructure. This unit cell should be small enough to account for local variations but large enough to include significant microstructural features. Once the unit cell is defined, specific boundary conditions, typically periodic boundary conditions, are applied to the unit cell to mimic the periodicity of the microstructure. These boundary conditions allow for the periodic repetition of the unit cell throughout the material. Next, the homogenisation procedure involves analysing the local behaviour of the unit cell using mathematical techniques like the method of multiple scales or asymptotic expansions. This analysis results in a series of solutions for different length scales, which represent the contributions of various microstructural features to the overall material response. With the results from the homogenisation procedure, the effective properties of the composite material can be derived. These effective properties represent the macroscopic behaviour of the composite at a larger length scale, and they are crucial for designing and analysing composite structures. In addition, the flow chart presented in Fig. 4 represents the homogenisation process.

Numerous analytical models have been developed to predict the electromechanical properties of piezoelectric composites through homogenisation techniques. Challagulla et al. [87] introduced an asymptotic homogenisation method to obtain complete properties of 2–2 layered composites with anisotropic constituents. They explored longitudinally and transversely layered variants for both large and small-volume systems. An extension of this method for 1–3 long-fibre piezoelectric composites with transversely isotropic constituents was presented by Bravo-Castillero et al. [88]. Variational bounds were provided by Bisegna et al. [89] to estimate homogenised properties, and Hori et al. [73] derived Hashin–Shtrikman type exact bounds. Nasedkin et al. [90] performed numerical studies on porous piezoelectric composites, using effective moduli theory based on the Hill–Mandel principle. They investigated properties of a piezoelectric matrix containing a spherical hole, analysing how increased metal fraction influences effective moduli. Georgiades et al. [91] developed a unit cell-based approach yielding expressions for effective elastic, piezoelectric, and thermal expansion coefficients. These universal expressions allow customisation of smart structures by adjusting material or geometric parameters. This methodology was applied to smart network-reinforced composites with orthotropic reinforcements and actuators. Silva et al. [36] employed topology optimisation and homogenisation to determine effective material properties. Vatanabe et al. [92] introduced another topology technique for designing functionally graded piezoelectric materials with superior energy harvesting performance. Li-Kun et al. [93] analytically and experimentally studied how properties of 1–3 piezo composites vary with material properties and volume fraction. Nasser et al. [94] used analytical and numerical approaches to determine effective electro-mechanical properties of macrofibre composites, finding that maximising the ratio between piezoelectric properties in different directions requires specific Young's modulus and Poisson's ratio values.

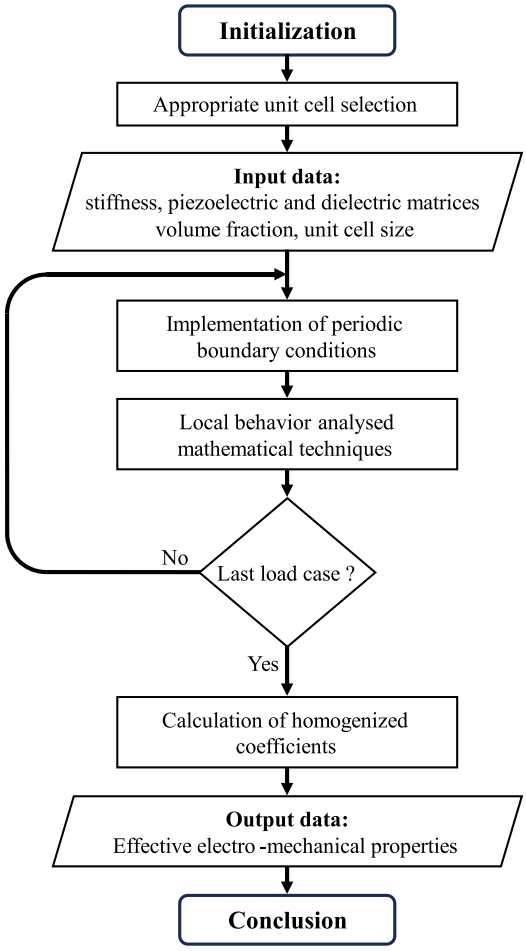

Fig. 4. Flow chart to process the homogenisation.

The research conducted by Berger et al. [95] delves into modelling 1–3 periodic composites, consisting of piezoceramic (lead zirconate titanate) fibres within a non-piezoelectric polymer matrix. Their focus lies on predicting effective coefficients for these transversely isotropic piezoelectric fibre composites, utilising the unit cell method. They provide two approaches for calculating these coefficients: an analytical method based on asymptotic homogenisation, and a numerical method using FEM. Ensuring periodicity by defining appropriate boundary conditions for the unit cell is of paramount importance.

Expanding upon this work, Berger et al. [96] continued their study on 1–3 periodic piezoceramic composites, exploring both square and hexagonal arrangements of cylindrical fibres [97]. They extended their method to include soft epoxy matrices [98]. Kari et al. [99] adopted a modified random sequential adsorption algorithm for creating unit cell models in unidirectional piezoelectric fibre composites with square and hexagonal fibre arrangements, using FEM-based numerical homogenisation to analyse the effects of fibre diameter and packing.

Iyer et al. [100] developed an analytical framework based on homogenisation for predicting electromechanical properties of periodic, particulate, and porous piezoelectric composites with anisotropic constituents. This involved expressions for effective moduli tensors of n-phase composites, considering inclusion shape and distribution. They found excellent agreement between their analytical predictions and results from 3D finite-element models.

Nasser et al. [101] employed the variational asymptotical method for unit cell homogenisation to design a unidirectional piezoelectric transducer, while Qin et al. [102] combined the boundary element method with homogenisation to determine effective material properties. Reda et al. [103] proposed a methodology involving oscillating functions for computing effective properties of layered piezoelectric materials. Caballero-Pérez et al. [104] applied asymptotic homogenisation to linear thermo-piezoelectric properties of ceramic matrix materials with periodic cylindrical pores, with potential for energy harvesting. Nasimsobhan et al. [105] determined flexoelectric properties using asymptotic expansion and proposed a general theory for stratified piezoelectric plates.

Numerical evaluations of effective properties for active piezoelectric fibre composites were conducted by De Medeiros et al. [106], while Wampo et al. [107] developed a generalised homogenisation model adaptable to various connectivity patterns for 2–2 and 1–3 piezo composites. Gerasimenko et al. [108] considered inhomogeneous polarisation's effect on effective properties of piezoelectric composites. Nasedkin et al. [109] proposed a reciprocity relation for predicting effective properties and validating with known values. Camarena et al. [110] employed analytical homogenisation to find effective

electro-mechanical properties of piezoelectric fibre composites, using recent structural mechanics insights.

A novel homogenisation method was introduced by Challagulla et al. [111], which is based on the diffused material interface technique [112], applicable to arbitrary inclusion shapes, and studied the influence of non-elliptical inclusions on the macrolevel electro-elastic response of periodic composites. This extensive body of work collectively advances the understanding and prediction of effective properties in various piezoelectric composite systems.

In the realm of composite materials, including distinct variations like periodic grids, composite shells, and textured composites, a plethora of studies parallel those previously mentioned. Researchers have undertaken comprehensive investigations into these multifaceted composite configurations, each tailored to specific design goals and material behaviours.

For instance, Hassan et al. [113] introduced a comprehensive micromechanical model for 3D smart composite structures featuring a periodic grid of generally orthotropic cylindrical reinforcements, which also possess piezoelectric behaviour. Using asymptotic homogenisation, they decoupled the complex boundary value problem into simpler unit cell problems, enabling the determination of effective elastic, piezoelectric, and thermal expansion coefficients. Practical examples, such as cubic and conical embedded grids and diagonally reinforced smart structures, were employed to illustrate the model's application.

In a similar vein, Challagulla et al. [114] developed a micromechanical model for analysing thin smart composite grid-reinforced shells with embedded periodic grids of generally orthotropic cylindrical reinforcements, potentially exhibiting piezoelectric properties. The asymptotic homogenisation technique was employed again, facilitating the determination of effective coefficients. This comprehensive approach was applied to examples like cylindrical reinforced smart composite shells and multi-layer smart shells [115]. Kalamkarov et al. [116] employed the asymptotic homogenisation method to analyse smart composite structures reinforced by a periodic grid of generally orthotropic cylindrical reinforcements with piezoelectric behaviour. Analytical expressions for effective elastic and piezoelectric coefficients were derived, covering cases with cubic, conical, and diagonal orientations. Saha et al. [117] extended the micromechanical model to encompass smart composite shells with periodically arranged embedded piezoelectric actuators and varying thickness. This complex problem was tackled using asymptotic homogenisation, leading to the determination of local fields and effective coefficients. Orthotropic constituent materials added complexity, but the model allowed tailoring effective properties for different applications through geometric and material parameter adjustments. Jayachandran et al. [118,119] integrated stochastic global optimisation with the homogenisation method to optimise ferroelectric ceramic microstructures for piezoelectric actuators. The influence of inner periodic architectural topology on effective piezoelectric properties was explored in [120], utilising the extended Hill–Mandel macrohomogeneity condition to evaluate homogenised electro-mechanical properties.

Hence, the analyses outlined above offer just a glimpse of the vast array of investigations made possible through the utilisation of Asymptotic Homogenization-Based models. As delineated in Table 1, these analyses underscore the extensive spectrum of research avenues that can be explored using this modelling approach. Each of the referenced studies presents a unique perspective within the realm of modelling and analysing piezoelectric composite materials. Furthermore, these studies provide an ideal platform for delving into an extensive array of research inquiries, showcasing the dynamic potential inherent in this field of study.

Though the several advantages of the asymptotic homogenisation over direct simulations of the entire microstructure, there are limitations to the applicability of the method. This assumes a periodic and regular microstructure, which may not be suitable for composites with irregular arrangements or strong spatial variations. The accuracy of the results heavily depends on the appropriate representation of the microstructure in the chosen unit cell. For reliable results, it is essential to carefully define the unit cell to capture the critical microstructural features accurately. Furthermore, asymptotic homogenisation is most effective for materials with small variations in material properties or low contrast materials. For composites with high contrast or exhibiting complex

Table 1
Analyses that can be performed using Asymptotic Homogenization-Based models.

Analyses	Description	Authors
Homogenisation analysis for piezoelectric composites	The applicability of the asymptotic homogenisation methodology to other types of compositions and piezoelectric material characteristics was explored.	Challagulla et al. [87]
Properties of anisotropic composite materials	The differences between longitudinally and transversely layered fibre compositions, as well as the implications of anisotropic variations in constituents was investigated.	Challagulla et al. [87] Bravo-Castillero et al. [88]
Estimation of electromechanical properties	The estimates of homogenised properties provided by different approaches for calculating limit and variational properties was compared.	Hori et al. [73] Bisegna et al. [89]
Modelling of porous piezoelectric composites	The changes in effective properties with varying metal fraction and examine the influence of porosity on piezoelectric characteristics was analysed.	Nasedkin et al. [90]
Customisation of smart structure properties	Universal expressions of effective coefficients were used to design smart structures with tailored properties, adjusting geometric and material parameters.	Georgiades et al. [91]
Materials optimisation for energy harvesting	Topology and functional optimisation techniques to design piezoelectric materials with superior performance for energy harvesting was explored.	Silva et al. [36] Vatanabe et al. [92]
Sensitivity analysis of composites	Investigation how electromechanical properties of 1–3 composites vary with volume fraction and the effects of different material properties was performed.	Li-Kun et al. [93]
Effects of fiber orientation in composites	The impact of fibre orientation and diameter on determining effective properties of these composites was analysed.	Kari et al. [99]
Comparison between analytical and numerical models	The predictions of the developed analytical model were validated with results from numerical finite element models in various configurations.	Iyer et al. [100]
Piezoelectric transducer design	The properties determined by the homogenisation method to optimise the design of unidirectional piezoelectric transducers was explored.	Nasser et al. [101]
Flexoelectric effect analysis	The relationship between flexoelectric effects and the layered response of piezoelectric plates was investigated.	Nasimsobhan et al. [105]
Modelling properties in periodic composites	The new homogenisation approach based on the diffuse material interface technique was used to understand how non-elliptical inclusion shapes affect macro-level electro-elastic properties.	Challagulla et al. [111]

nonlinear behaviour, more advanced homogenisation techniques may be required to achieve accurate results.

3.4. Summary

The Table 2 provide a comprehensive summary of analytical models designed to predict the electromechanical behaviour of piezoelectric composites is presented, accounting for material characteristics and the specific composite types studied. Notably, a predominant focus is observed on long-fibre composites exhibiting either transversely isotropic or anisotropic properties. However, a distinct pattern emerges when considering Eshelby-type models. These models have been sparingly employed in the exploration of long-fibre composites with anisotropic properties. This trend can be attributed to the inherent limitations of Eshelby-Type Models in accurately predicting the effective transverse modulus. These models primarily prioritise volume fraction, which limits their applicability in this aspect. As a result, Eshelby-Type Models find constrained utility in studying composites involving particles or porous, with Micromechanics-Based Models and Asymptotic Homogenization-Based Models assuming prominence in such scenarios. A similar trend is evident to predict the electromechanical behaviour of laminated composites.

The advantages and disadvantages of three different types of analytical models (Micromechanics-Based Models, Eshelby-Type Models, and Asymptotic Homogenization-Based Models) used in material science and engineering for predicting the behaviour of piezoelectric composite materials are outlined in Table 3.

Micromechanics-Based Models offer simplicity and the ability to predict material properties in specific directions. They are particularly effective for certain types of composites and anisotropic materials. These models can guide optimisation efforts and predict composite behaviour under various loading conditions. However, they may struggle with transverse properties, matrix-dominant scenarios, and high anisotropy, limiting their accuracy.

Eshelby-type models excel at accurately estimating the properties of composites with specific reinforcement shapes and materials,

Table 2
A summary of the analytical models developed to predict the electromechanical response of piezoelectric composites.

Analytical models	Material behaviour	Particulate composites or porous within composites	Long-fibre composites or periodic grid	Laminate composites
Micromechanics-based models	TI		Tan et al. [49] (2001) Malik et al. [50] (2003) Kar-Gupta et al. [47] (2007) Kumar et al. [51] (2009) Aimmanee et al. [20] (2020) Singh et al. [53] (2022)	
	A	Hashmimoto et al. [37] (1986) Banno et al. [38] (1987) Levassort et al. [40–42] (1997–1999) Bowen et al. [46] (2003) Odegard et al. [54] (2004) Dinzart et al. [55] (2009)	Hashmimoto et al. [37] (1986) Banno et al. [38] (1987) Levassort et al. [40–42] (1997–1999) Tan et al. [49] (2001) Bowen et al. [46] (2003) Kar-Gupta et al. [47] (2007)	Hashmimoto et al. [37] (1986) Banno et al. [38] (1987) Levassort et al. [40–42] (1997–1999) Topolov et al. [45] (2009) Kar-Gupta et al. [48] (2013)
Eshelby-type models	TI	Dunn et al. [68,121,122] (1993–1996) Wang et al. [123] (1994) Mikata et al. [70] (2001)	Dunn et al. [69,121,122] (1993–1996) Wang et al. [123] (1994) Chen et al. [124] (1996) Mikata et al. [64] (2000) Odegard et al. [54] (2004) Dinzart et al. [55] (2009) Chambion et al. [125] (2011) Dai et al. [126] (2012) Malakooti et al. [75] (2012) Rodríguez et al. [76] (2022) Chen et al. [78,79] (2022–2023)	Jacquet et al. [84] (2000)
	A	Hori et al. [73] (1998) Fakri et al. [71] (2003) Hasanzadeh et al. [77] (2019) Rodriguez et al. [80] (2019)	Hori et al. [73] (1998)	Lee et al. [127] (1990) Hori et al. [73] (1998) Jacquet et al. [84] (2000) Chen et al. [72] (2002) Trzepieciński et al. [128] (2018)
Asymptotic homogenization-based models	TI		Bisegna et al. [89] (1997) Silva et al. [36] (1998) Bravo et al. [88] (2001) Rodríguez et al. [129] (2001) Berger et al. [95–98] (2005–2006) Kari et al. [99] (2007) Li-Kun et al. [93] (2008) Medeiros et al. [106] (2015) Wampo et al. [107] (2022)	Otero et al. [130] (2005) Georgiades et al. [91] (2006) Wampo et al. [107] (2022)
	A	Qin et al. [102] (2004) Iyer et al. [100] (2014) Gerasimenko et al. [108] (2019) Caballero-Pérez et al. [104] (2020) Nasedkin et al. [109] (2020) Challagulla et al. [111] (2023)	Bisegna et al. [89] (1997) Saha et al. [117] (2007) Hassan et al. [113] (2009) Georgiades et al. [115] (2010) Nasser et al. [94] (2011) Kalamkarov et al. [116] (2012) Iyer et al. [100] (2014) Camarena et al. [110] (2019) Challagulla et al. [111,114] (2010, 2023)	Georgiades et al. [115] (2010) Nasser et al. [101] (2016) Camarena et al. [110] (2019) Reda et al. [103] (2020) Nasimsobhan et al. [105] (2022) Challagulla et al. [87,111] (2009, 2023)

Legend: TI – Transversely Isotropic; A – Anisotropic.

Table 3
An overview of the analytical models' advantages and disadvantages.

Analytical models	Advantages	Disadvantages
Micromechanics-based models	• For 1–3 type composites, the material properties in the longitudinal direction are well-predicted [47]. • For anisotropy material, the material behaviour and properties are well predicted. • Provide useful information for optimising the composite performance by selecting the optimal microstructure and properties of composite constituents [49]. • Simplicity and ability to determine the effective coefficients without excessive computational efforts [51]. • Predict the complete behaviour of the piezoelectric composite subjected to thermo-electro-mechanical loading [51].	• The 0–3 and 3–3 type composites showed to be less sensitive to the anisotropy factor [46]. • For 1–3 type composites, the material properties in the transverse direction are underpredicted for matrix-dominant [47]. • For 2–2 type composites, the material properties along a direction perpendicular to the layer interface are influenced by the properties of the 'softer' phase [48]. • Strong dependence of effective properties on Young's modulus of the matrix material [51].
Eshelby-type models	• Ellipsoidal reinforcement shapes are employed to simulate thin lamina to continuous fibre at spherical particles [66]. • Precision on the precise electro-elastic property estimation for piezoelectric composites [66]. • Porosity, shape and concentration are covered in piezoelectric ceramics with any material symmetry [68]. • Elliptical crack-like inclusions, regardless of aspect ratio, share the same piezoelectric Eshelby tensor [64]. • Self-consistent and Mori-Tanaka methods yield acceptable results, former tends to overestimate. • The derived expressions are crucial for 2D inclusion problems in piezoelectric solids using an equivalent inclusion approach [121]. • Tensors solve piezoelectric problems like defects, fractures, and composites [121].	• Interactions among inclusions at finite volume fractions are disregarded. • The dilute approach becomes unreliable at high volume fractions, possibly an asymptotic limit of the models. • Numerical results reveal significant effects of volume fraction, aspect ratio, and orientation on electro-elastic modulus. • The Eshelby-type approach doesn't address laminate issues. • Mori-Tanaka approach struggles to predict effective transverse modulus ($C_{11}^{eff} = C_{22}^{eff}$) due to its focus solely on volume fraction[126].
Asymptotic homogenization-based models	• Computational expenses are significantly reduced for large-scale composite analysis. • Efficient estimation of effective material properties under various loading conditions, allowing designers to optimise material performance. • Complex microstructures can be handled, including composites with periodic arrangements and repeating patterns. • When applied to smart composites, these models predict both local and global effective properties of the structure [113]. • These models allow tailoring of effective coefficients of smart grid-reinforced structures by adjusting material or geometric parameters [115]. • Successful application to analyse complex structures with embedded actuators and varying thickness [117].	• These models' assumption of a periodic and regular microstructure restricts its applicability to materials with irregular arrangements or strong spatial variations. • Accurate results heavily rely on appropriately defining the RVE to capture critical microstructural features. • Effective for materials with small property variations or low contrast. It may struggle with high-contrast composites or those exhibiting complex nonlinear behaviour.

particularly in piezoelectric composites. They offer insight into various geometries and symmetries, but they may not account for interactions among inclusions at high volume fractions. These models are powerful for certain problems like defects and fracture, but they might not fully address laminate issues or transverse modulus predictions due to certain simplifications.

Asymptotic Homogenization-Based Models stand out for efficiently estimating properties of complex microstructures, allowing optimisation and analysis of large-scale composites. They are versatile in handling various loading conditions and materials with periodic arrangements. However, they are limited by their assumption of regular microstructures and may struggle with highly contrasting or nonlinear materials.

In summary, each model type has its strengths and limitations, and their appropriateness depends on the specific characteristics of the piezoelectric composite materials being studied. Researchers and engineers should choose the model that aligns best with their material's properties and the analysis goals at hand.

4. Numerical models: finite element models

Piezoelectric composites often exhibit intricate microstructures, and their behaviours can be influenced by a multitude of factors, including geometric irregularities, anisotropy, and complex boundary conditions. FEM is frequently employed to comprehensively reconstruct the intricate microstructure of composite materials. This involves capturing the heterogeneous spatial distribution of particles or fibres, the irregular shapes of these particles, and the anisotropic properties within them. Several effective numerical models, grounded in FEM, have been devised to investigate the electromechanical properties of piezoelectric composites. Understanding and accurately predicting the mechanical and electroelastic properties of such materials pose significant challenges in engineering analysis. Numerical techniques have emerged as indispensable tools in the field of materials science and engineering, being FEM one of the most widely employed numerical methods in simulating the behaviours of piezoelectric composites. This introduces the fundamental concepts and motivations behind the utilisation of FEA in the context of piezoelectric composites, discussing its strengths and limitations.

The Representative Volume Element (RVE) is a fundamental technique in materials science and mechanics, employed to characterise the mechanical and physical properties of heterogeneous materials. Its primary purpose is to simplify the analysis of complex materials by considering a small, yet statistically representative portion known as the RVE. This approach allows researchers to make predictions about the material's macroscopic behaviour based on the properties of this microscale unit [131].

One of the key principles of the RVE method is the idea of statistical representation. The chosen RVE must strike a balance - it should be small enough to be computationally tractable yet large enough to encompass a representative sample of the material's microstructure. In doing so, the RVE aims to capture the essential features of the material's heterogeneity, which can vary widely across different materials.

Homogenisation is a central concept in the RVE method. It involves subjecting the RVE to various loadings and boundary conditions to study its electromechanical response. Through this process, researchers seek to determine effective or homogenised material properties. These

effective properties can then be applied at the macroscopic scale to simplify the analysis of heterogeneous materials, such as composites, foams, and porous media.

The size and shape of the RVE are critical considerations. They depend on the specific material being studied and the features of interest. For instance, in the context of composite materials, the RVE may represent a repeating unit of the material's microstructure, such as the arrangement of fibres in a fibre-reinforced composite.

RVE's Methods based on the Finite Element (FE) and analytical methods both offer distinct advantages and disadvantages. The analytical approach excels in modelling statistical distributions and demands considerably less computational time, often taking just a few seconds to complete. On the other hand, FE analysis, although more computationally intensive (taking a few minutes), is particularly suited for estimating the effective properties of composites with predetermined periodic fibre or particle distributions. Moreover, FE analysis can accommodate more intricate boundary conditions [132].

Recent advancements have seen the combination of the RVE method with macroscopic mechanical analysis, yielding promising results. This hybrid approach has been successfully employed in modelling the sensor capabilities of a prototype impact sensor. For a comprehensive understanding of the sensor's design, experimentation, and modelling [132].

The field of numerical modelling for piezoelectric composite materials is a cornerstone of modern engineering and materials science. It enables us to understand and predict the behaviour of complex materials composed of distinct phases, such as reinforced composites, metal matrix composites, or multiphase polymers. In this realm, the journey begins with the creation of an RVE, a miniature sample that encapsulates the essential structural features of the entire composite. Assigning material properties, meshing, applying constraints, and imposing loading conditions are all integral parts of this intricate process. Through numerical simulations, it is possible to gain insights into how these materials respond to mechanical, thermal, or electrical stimuli, ultimately extracting effective properties critical for designing and engineering innovative composite materials for a wide range of applications, from aerospace components to biomedical devices. This theme explores the step-by-step intricacies of numerical modelling, shedding light on the fascinating world of composite materials and their multifaceted behaviour.

Building an RVE:

- The first crucial step in modelling composite materials is creating an RVE. This RVE represents a small portion of the composite material, and its properties and behaviour should accurately reflect those of the entire composite.
- The RVE is typically chosen to be small enough to make computational simulations manageable but large enough to capture the key features of the composite's microstructure.

Assigning Material Properties to the Matrix and Reinforcement:

- In piezoelectric composite materials, there are usually two phases: the matrix (often a polymer or metal) and the reinforcement (typically fibres or particles) or porous. It is essential to assign appropriate material properties to these phases within the RVE.
- These material properties include mechanical properties (e.g., Young's modulus, Poisson's ratio), electrical properties (such as conductivity or permittivity), piezoelectric properties and, in some cases, thermal properties.

Creating a Periodic Mesh on Opposite Surfaces of the RVE:

- To apply periodic boundary conditions accurately, it is necessary to generate a mesh on the opposite surfaces of the RVE. This mesh should match the corresponding nodes on opposite surfaces.
- The periodicity ensures that any physical effects observed within the RVE can be extrapolated to the entire composite material accurately.

Applying Constraint Equations to Nodes and Boundary Conditions:

- Constraint equations are mathematical relations that describe the behaviour of nodes within the RVE (Fig. 5). These equations often involve degrees of freedom (DOFs) related to translations and possibly other properties such as electric potential.
- Each node within the RVE typically has multiple DOFs, and these equations enforce the relationships between nodes due to the constraints imposed by the composite's microstructure.

Determination of Effective Coefficients Using Loading Conditions:

- The primary goal of modelling composite materials is to determine their effective properties. This is achieved by applying external loading conditions, such as mechanical strains or electric fields, to the RVE.
- By analysing the response of the RVE to these loading conditions, effective material properties like the effective Young's modulus, piezoelectric properties, effective electrical conductivity, or effective thermal conductivity can be determined.
- The choice of loading conditions should align with the specific properties of interest and the expected use of the composite material.

In summary, implementing numerical models for composite materials involves creating a representative sample, assigning material properties, ensuring periodicity, applying constraints and boundary conditions, and finally, determining the effective properties through

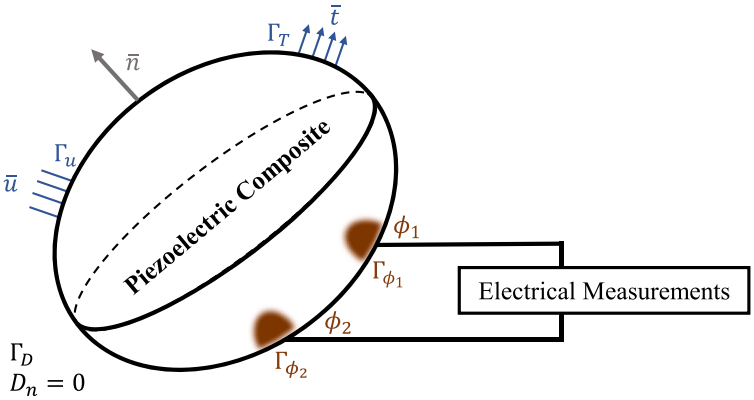

Fig. 5. Piezoelectric composites and boundary conditions.

appropriate loading conditions. This iterative process is crucial for accurately simulating the behaviour of composite materials in various applications [133,134].

In the realm of electro-mechanical modelling, engineers and scientists often grapple with the choice between linear and nonlinear models, each offering a unique set of advantages and disadvantages.

Linear electro-mechanical models, with their precision in predicting linear responses, prove invaluable for understanding materials' behaviours under moderate electric fields. Their simplicity and ease of application make them ideal for straightforward analyses and control systems where linearity suffices. Moreover, their analytical solutions empower researchers to derive mathematical insights, facilitating parameter estimation for experimental setups.

On the other hand, nonlinear electro-mechanical models shine when realism is paramount. They accurately represent materials' responses under intense electric fields, capturing phenomena like polarisation saturation and hysteresis. These models excel in predicting complex behaviour, such as polarisation switching and domain wall motion, vital in practical applications. Additionally, they offer flexibility in optimising material performance and tailoring it to specific application requirements.

However, it is essential to weigh these advantages against the complexities involved in employing nonlinear models. Their computational demands and the intricate nature of modelling nonlinearities can pose challenges. In contrast, linear models may fall short in representing real-world behaviour when dealing with large electric fields and nonlinear responses.

Ultimately, the choice between models with linear and nonlinear electro-mechanical behaviour models hinges on the specific application's demands and the level of accuracy required. Engineers and researchers must carefully consider these factors to select the most suitable modelling approach for their particular endeavours.

4.1. Linear electro-mechanical behaviour

The constitutive modelling of linear piezoelectric materials is an essential aspect of understanding their behaviour and predicting their response to external stimuli. Eqs. (44) represents a mathematical formulation that describes the relationship between the various physical properties and quantities associated with linear piezoelectric materials. In linear piezoelectric materials, which are often crystalline materials like quartz or certain ceramics [3,19,135], there is a linear relationship between mechanical stress (T_{ij}), electric field (E_i), strain (S_{ij}), and electric displacement (D_i). This linear relationship is described by the constitutive Eq. (2).

To characterise the behaviour of piezoelectric composites, the conventional electro-elastic equations in their linearised form can be adopted, focusing on infinitesimal strains and potential gradients [136]. In the context of piezoelectric composites, it is common to incorporate electrodes that establish a connection between the piezoelectric material and the electric circuit, as depicted in Fig. 5. An example displayed in Fig. 5, it can be possible to briefly express these equations as shown in Eqs. (44). Within the equation of motion, the stress tensor (T_{ij}) is a key factor, while the displacement (u_k) and material density (ρ) play their roles. As for the charge equation, it involves the electrical displacement (D_i), infinitesimal strain (S_{ij}), electrical field (E_i), and potential (ϕ). The linear constitutive equations encompass several quantities: C^{E}_{ijkl} signifies stiffness under a constant electrical field, d_{kij} notes piezoelectric stress coefficients, and ε^{S}_{ik} signifies the dielectric matrix assessed under constant strain conditions.

$$
\begin{cases}
T_{jk,\,j} = \rho \ddot{u}_k \text{ in } \Omega \\
D_{i,\,i} = 0 \text{ in } \Omega \\
S_{ij} = \dfrac{u_{i,j} + u_{j,i}}{2} \\
E_i = -\phi_i \\
T_{ij} = C^{E}_{ijkl}\, S_{kl} - d_{kij} E_k \\
D_i = d_{ikl}\, S_{kl} + \varepsilon^{S}_{ik}\, E_k \\
\Delta\phi = RI \\
u_i = \overline{u_i} \text{ on } \Gamma_u \\
t_i = T_{ji} n_j \text{ on } \Gamma_T \\
\phi = \overline{\phi_1} \text{ on } \Gamma_{\phi_1} \\
\phi = \overline{\phi_2} \text{ on } \Gamma_{\phi_2} \\
D_j n_j = 0 \text{ on } \Gamma_D
\end{cases}
\tag{44}
$$

The circuit equation interrelates the disparity in potential with the resistance (R) and the electric current (I) that traverses through it. When it comes to boundary conditions, there are the customary prescribed displacement conditions (u_{oi}) and traction conditions (t_i) on the respective domain boundary Γ_u and Γ_T. Simultaneously, there are specified potential conditions $\overline{\phi_i}$ and charge conditions $q = 0$ on Γ_{ϕ_i} and Γ_D, correspondingly, as illustrated in Fig. 5. It is worth noting that the surfaces marked as Γ_{ϕ_i} correspond to the electrode surfaces, and the composite surface, denoted by $\Gamma = \Gamma_{\phi_1} \cup \Gamma_{\phi_2} \cup \Gamma_D = \Gamma_u \cup \Gamma_T$, coincides with the merger of Γ_u and Γ_T.

In addition, the Einstein summation convention is employed for summation over repeated indices and the notation $\alpha_{i,j}$ represents partial derivatives $\frac{\partial \alpha_i}{\partial x_j}$ for spatial coordinates. Each electrode retains a constant electrical potential on the surface marked as Γ_{ϕ_i}.

The amount of unbound electric charge that moves across the surface Γ_{ϕ_i} is determined by the formula presented in Eq. (45). When this unbound electric charge changes over time, it gives rise to an electric current called I, which flows outward from the electrode. This relationship is precisely described by Eq. (46).

$$
Q_e = \int_{\Gamma_{\phi_i}} - n_i D_i \, d\Gamma \tag{45}
$$

$$
I = -\dot{Q}_e \tag{46}
$$

Numerous research studies have delved into the analysis of electro-mechanical behaviours in functionally graded piezoelectric structures. The majority of these investigations have primarily concentrated on linear electro-mechanical responses, which are applicable when these structures experience relatively modest electric field inputs. Examples of these analytical and numerical (finite element) investigations on the behaviour of functionally graded piezoelectric structures can be found in works such as Hauke et al. [137], Wang et al. [138], among others [75, 139–142].

In one notable study, Carbonari et al. [141] employed a topology optimisation approach to identify the optimal variations and polarisation axes in functionally graded bimorph beams, with a focus on maximising lateral displacements as the performance metric. They employed a combination of piezoelectric ceramics and metals as the constituent materials in these functionally graded bimorph beams. Additionally, Vatanable et al. [143] also utilised topology optimisation techniques to investigate the impact of patterned gradations on the design of functionally graded piezoelectric beams (FGPBs) intended for energy harvesting applications.

Several studies have explored the utilisation of smooth and monotonic spatial functions to ascertain the overall electro-mechanical

properties within graded piezoelectric materials. Examples of such research include works by Bhangale et al. [144], Huang et al. [145], Panda et al. [146], and Yang et al. [147]. Employing monotonic functions to determine material properties along the graded region is often found convenient, especially when considering linear electro-mechanical responses. In some composite materials, effective electro-mechanical properties can be reasonably approximated by applying the rule of mixture, which combines the properties of individual constituents.

4.2. Nonlinear electro-mechanical behaviour

Piezoceramics play a crucial role in various technological applications, particularly in the realm of sensors and actuators. To harness their full potential, these materials undergo a process known as polarisation, which involves subjecting them to a high electric field at elevated temperatures, typically exceeding the coercive electric field threshold. This polarisation step is essential for optimising their performance [148].

In many actuator applications, polarised piezocomposites are exposed to high electric fields, leading to intriguing nonlinear electro-mechanical responses. These responses are characterised by the complex interplay between electrical and mechanical properties. To understand and analyse these behaviours, Tiersten [149] introduced a constitutive model tailored to capture the intricacies of polarised piezoceramics when subjected to large electric fields but lower than the coercive electric field of the piezoceramics.

One notable nonlinear electromechanical phenomenon in piezoceramics is hysteretic polarisation switching. This effect occurs when ferroelectric materials experience cyclic electric fields with amplitudes surpassing the coercive electric field. The polarisation switching response is inherently nonlinear, as it involves the material transitioning between different polarisation states during each cycle of the electric field.

Tiersten's [149] nonlinear constitutive model, designed for polarised piezoceramics exposed to large electric fields and experiencing relatively small strains, is expressed in Eq. (47). This model aims to mathematically describe the intricate relationship between the electrical field E_i, mechanical strain S_{ij}, mechanical stress T_{ij} and electric displacement D_i, providing a valuable tool for understanding and predicting the behaviour of these materials under such conditions.

$$\begin{cases} S_{ij} = s_{ijkl}\, T_{kl} + d_{kij} E_k + \frac{1}{2} f_{klij} E_l E_k \\ D_i = d_{ikl} T_{kl} + \varepsilon^{S}_{ik}\, E_k + \frac{1}{2} \chi_{ijk} E_k E_j \end{cases} \tag{47}$$

Material properties are essential in this context. They include elastic compliances represented as s_{ijkl}, which are determined under constant electric fields. Additionally, it is possible to observe, third- and fourth-order piezoelectric strain coefficients, d_{ijk} and f_{ijkl}, respectively, which are determined under constant stresses. Furthermore, it was considered second- and third-order dielectric coefficients ε^{S}_{ij} and χ_{ijk}, which are calibrated under constant stresses.

To account for the nonlinear response of polarised piezoelectric materials in the presence of high electric fields, higher-order terms of the electric field are introduced. This enables us to better describe and analyse the behaviour of these materials in such conditions.

In applications involving actuation, piezoelectric composites are often subjected to high electric fields, resulting in nonlinear electro-mechanical responses. Various experimental studies, such as those conducted by Kouvatov et al. [150] and Jin et al. [151], have demonstrated nonlinear behaviours and hysteresis in piezoelectric functionally graded beams when exposed to significant electric fields. These studies revealed nonlinear polarisation and switching responses in these beams under such conditions. Additionally, Takagi et al. [152] highlighted nonlinear electro-mechanical responses in polarised functionally graded beams when subjected to large electric fields.

When one or more constituents within these composites exhibit nonlinear behaviour, simply applying a rule of mixture may not suffice to predict the overall nonlinear responses of the composites. To address this, several micromechanics models have been widely employed [62,124,153–158]. These models encompass diverse microstructural arrangements and account for different constituent behaviours, allowing for the prediction of both linear and nonlinear electro-mechanical responses in piezoelectric composites.

However, it's worth noting that the current understanding of analysing nonlinear electro-mechanical responses, particularly concerning polarisation and hysteresis behaviours, in functionally graded piezoelectric structures, remains somewhat limited. Although Kouvatov et al. [150] have examined the nonlinear hysteretic responses of functionally graded beams, their approach involved discretising the beam into multiple layers of homogeneous materials and employing higher-order polynomial functions to capture the nonlinear hysteretic polarisation within each electro-active layer of the functionally graded beam. Nevertheless, the precise methodology they used to incorporate these hysteretic responses using higher-order polynomial functions remains somewhat unclear. By examining the nonlinear responses of multi-scale models, Lin et al. [159] further, contribute to the clarification of these results.

4.3. Representative volume element method

The RVE is a crucial tool in materials science and mechanics, used to assess heterogeneous materials' properties. It simplifies complex material analysis by examining a small, statistically representative portion. This allows researchers to predict macroscopic behaviour based on microscale properties. Key principles include achieving statistical representation while balancing computational feasibility and capturing essential heterogeneity features. Homogenisation is central, involving subjecting the RVE to various conditions to determine effective material properties for macroscopic-scale analysis of heterogeneous materials like composites and foams. RVE size and shape depend on the material and specific features of interest, such as representing a repeating unit in composite materials.

The applications of the RVE method are diverse and span various scientific disciplines. It is used to predict the effective electromechanical properties of composite materials, which often exhibit complex microstructures [52,54,96,134]. Additionally, the method finds application in the analysis of porous media [20,90,104,160–163].

However, the RVE method does come with its set of challenges. Selecting an appropriate size and shape for the RVE can be non-trivial, as it necessitates a careful balance between capturing relevant microstructural features and maintaining computational manageability. Extracting accurate boundary conditions for the RVE can also be complex, especially when dealing with interactions between neighbouring material phases. Additionally, achieving convergence and accuracy in simulations, particularly for highly heterogeneous materials, often demands significant computational resources.

In conclusion, the RVE method is an indispensable tool for characterising heterogeneous materials. Simplifying complex microstructures into manageable units for analysis, empowers researchers to make predictions about macroscopic behaviour and properties, offering

valuable insights into the design and understanding of materials with diverse applications.

4.3.1. Periodic arrangement of reinforcements

In the realm of actual piezoelectrical composite materials, the particles or fibres often exhibit intricate, irregular shapes and are irregularly dispersed. However, for the sake of analytical convenience and to facilitate a more tractable mathematical framework, a simplifying assumption can be made. Specifically, ceramic particles can be approximated as possessing spherical geometry, and their distribution within the matrix can be considered uniform. Likewise, fibres are approximated as cylindrical and are also assumed to be uniformly distributed.

To harness the analytical power of this simplified model, the framework of the periodic microfield approach is adopted. This approach hinges on the utilisation of RVE's, as illustrated in Fig. 3, to represent the repeating structural motifs within the composite material. A well-defined coordinate system is established, with its origin situated at the centre of a ceramic particle. The three-axis aligns precisely with the direction of particle alignment and the direction of tensile loading. In this setup, the particles are represented as perfect spheres with a characteristic radius. These spheres are systematically spaced apart by a specific distance in the direction of loading and the transverse direction, as specified in the reference [164].

This deliberate simplification and systematic arrangement of particles and fibres into uniform geometrical shapes within RVEs enable researchers and engineers to apply rigorous mathematical methodologies to analyse the composite's mechanical and electromechanical properties. This approach, while inherently idealised, serves as a valuable foundation for investigating the behaviour of composite materials in controlled, yet representative, conditions.

4.3.2. Random arrangement of reinforcements

The random microstructure under consideration is characterised by the presence of piezoelectric particles or fibres that are deliberately positioned in the matrix, as depicted in Fig. 6. The arrangement of these particles or fibres is achieved through a controlled process that leverages computational tools such as ANSYS Parametric Design Language, Matlab, and various other analytical software packages [99,125,165]. This meticulous procedure for generating a three-dimensional composite microstructure, featuring a random distribution of these particles or fibres within the matrix, unfolds as follows:

- **Generation of Random Cube Centres:** In the initial step, random coordinates for cube centres are determined. These coordinates serve as pivotal reference points within the matrix, forming the basis for subsequent particle or fibre placement.
- **Random Orientation of Symmetry Axes:** Following the establishment of cube centres, the symmetry axes of these cubes are subjected to a randomised orientation. This orientation is precisely defined using mathematical constructs known as versors, which govern the direction and alignment of each cube within the composite material.
- **Construction of Particles or Fiber:** With the cube centres and their orientation in place, the actual particles or fibres are meticulously constructed within the matrix. This construction adheres to a fundamental equation, as elucidated in reference [166], which encapsulates the intricate interplay of material properties and geometrical considerations.

This methodical approach ensures the creation of a 3D composite microstructure that faithfully replicates the randomness inherent in real-world materials, thus enabling a comprehensive exploration of their mechanical and electromechanical properties for scientific analysis and engineering applications.

4.4. Theory of periodic boundary conditions

Composite materials can be effectively characterised by representing them as a periodic array of RVEs. To accurately simulate the behaviour of the composite, it is necessary to apply periodic boundary conditions to the RVE models [167,168]. This means that the deformation mode of each RVE in the composite remains consistent, and there is no separation or overlap between neighbouring RVEs. The application of periodic boundary conditions given by Sun et al. [168] ensures that the RVEs at the boundaries of the composite adhere to this behaviour. In essence, these conditions establish the necessary constraints to maintain the periodicity and homogeneity of the composite structure, allowing for reliable analysis and prediction of its mechanical response.

In Eq. (48), $\bar{S}_{ij}$ represents the average strains, while v_i represents the periodic part of the displacement components, which signifies the local fluctuation, specifically on the boundary surfaces. The values of v_i are generally unknown and depend on the applied global loads. The indices i and j denote the three-dimensional coordinate directions, ranging from 1 to 3. To derive a more explicit form of periodic boundary conditions suitable for square RVE models, it is possible to refine the general expression of the Eq. (48). Considering the RVE depicted in Fig. 7b, the displacements on a pair of opposite boundary surfaces, with their normal aligned along the x_j axis can be expressed as the Eq. (49) and Eq. (50). In the Eq. (49) and Eq. (50), the index 'K^+' denotes displacement along the positive x_j direction, while 'K^-' represents displacement along the negative x_j direction, corresponding to the surfaces A^-/A^+, B^-/B^+, and C^-/C^+ (Fig. 7a).

$$u_i = \bar{S}_{ij} x_j + v_i \tag{48}$$

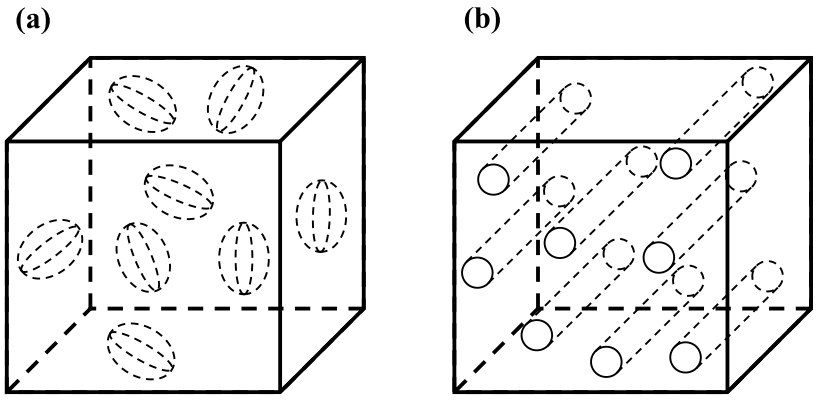

Fig. 6. Random arrangement of reinforcements: (a) particles and (b) fibres.

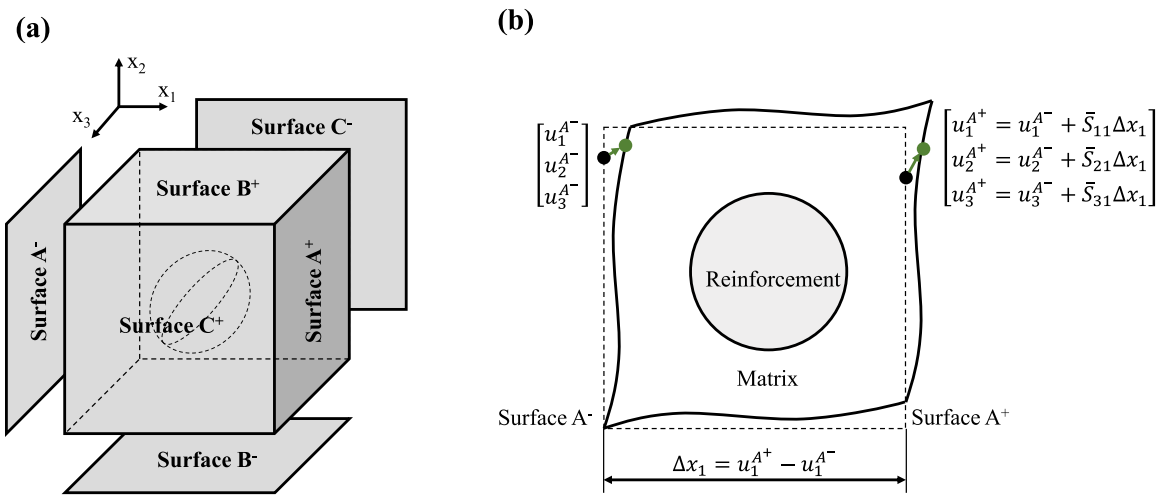

Fig. 7. Schematic diagram of an RVE: (a) surfaces and (b) surface displacements.

$$u_i^{K+} = \bar{S}_{ij} x_j^{K+} + v_i^{K+} \tag{49}$$

$$u_i^{K-} = \bar{S}_{ij} x_j^{K-} + v_i^{K-} \tag{50}$$

The Eq. (49) and Eq. (50) demonstrate that the local fluctuations (v_i^{K+} and v_i^{K-}) around the average macroscopic value are identical on opposing faces due to the periodic conditions of the RVE. Hence, the difference between the two equations lies in the applied macroscopic strain condition (Eq. (51)). By analysing and understanding these relationships, it was possible to establish a clearer understanding of how periodic boundary conditions manifest within square RVE models.

$$u_i^{K+} - u_i^{K-} = \bar{S}_{ij}\left(x_j^{K+} - x_j^{K-}\right) \tag{51}$$

The imposition of periodic boundary conditions on the electric potential is accomplished by incorporating the applied macroscopic electric field condition. This concept is analogous to what can be observed in the Eq. (52), allows for the simulation or analysis of electrostatic systems in a finite computational domain. By effectively 'wrapping' the domain at its boundaries, the macroscopic electric field condition ensures that the electric potential remains continuous and consistent throughout the entire periodic structure.

$$\Phi^{K+} - \Phi^{K-} = \bar{E}_i\left(x_j^{K+} - x_j^{K-}\right) \tag{52}$$

It is a common assumption that the average mechanical and electrical properties of an RVE are representative of the average properties of the entire composite material. In other words, by considering a suitably sized RVE, one can effectively capture the macroscopic behaviour of the composite material under study. This approach is particularly useful for predicting the overall mechanical and electrical response of composite materials without the need to simulate the entire complex microstructure. To define the average stresses and strains in the RVE, it is used Eq. (53) and Eq. (54). These equations quantify the average mechanical response within the RVE, allowing us to understand how the composite material will behave under mechanical loading. The volume of the periodic RVE, denoted as V, plays a crucial role in computing these averages, ensuring that the results are appropriately scaled to the overall composite.

$$\bar{S}_{ij} = \frac{1}{V}\int_V S_{ij} dV \tag{53}$$

$$\bar{T}_{ij} = \frac{1}{V}\int_V T_{ij} dV \tag{54}$$

Similarly, for the average electric fields and electrical displacements within the composite material, it is used the Eq. (55) and Eq. (56). These equations govern the macroscopic electrical behaviour, elucidating how the composite material responds to an applied electric field. By considering the electric properties within the RVE and scaling them based on its volume V, it was possible to effectively predict the overall electrical characteristics of the composite, providing valuable insights into its functional behaviour.

$$\bar{E}_i = \frac{1}{V}\int_V E_i dV \tag{55}$$

$$\bar{D}_i = \frac{1}{V}\int_V D_i dV \tag{56}$$

4.5. Calculation methods for the effective coefficients

The relationship between strain and charge for materials belonging to the tetragonal and hexagonal crystal systems, such as poled piezoelectric ceramics like PZT (lead zirconate titanate) or $BaTiO_3$, is described by Eq. (57) (ANSI IEEE 176). This equation captures both the converse piezoelectric effect, where strain is generated by an applied electric field, and the direct piezoelectric effect, where charge is generated by applied strain [169]. Additionally, in the case of orthotropic piezoelectric composites, the stiffness matrix, piezoelectric matrix (the composite was polarised in 3) and dielectric matrix undergo simplification, resulting in 15 independent coefficients.

$$\begin{bmatrix} \bar{T}_{11} \\ \bar{T}_{22} \\ \bar{T}_{33} \\ \bar{T}_{23} \\ \bar{T}_{31} \\ \bar{T}_{12} \\ \bar{D}_1 \\ \bar{D}_2 \\ \bar{D}_3 \end{bmatrix} = \begin{bmatrix} C_{11}^{eff} & C_{12}^{eff} & C_{13}^{eff} & 0 & 0 & 0 & 0 & 0 & -d_{13}^{eff} \\ C_{12}^{eff} & C_{22}^{eff} & C_{23}^{eff} & 0 & 0 & 0 & 0 & 0 & -d_{13}^{eff} \\ C_{13}^{eff} & C_{23}^{eff} & C_{33}^{eff} & 0 & 0 & 0 & 0 & 0 & -d_{33}^{eff} \\ 0 & 0 & 0 & C_{44}^{eff} & 0 & 0 & 0 & -d_{15}^{eff} & 0 \\ 0 & 0 & 0 & 0 & C_{55}^{eff} & 0 & -d_{15}^{eff} & 0 & 0 \\ 0 & 0 & 0 & 0 & 0 & C_{66}^{eff} & 0 & 0 & 0 \\ 0 & 0 & 0 & 0 & d_{15}^{eff} & 0 & \varepsilon_{11}^{eff} & 0 & 0 \\ 0 & 0 & 0 & d_{15}^{eff} & 0 & 0 & 0 & \varepsilon_{22}^{eff} & 0 \\ d_{13}^{eff} & d_{13}^{eff} & d_{33}^{eff} & 0 & 0 & 0 & 0 & 0 & \varepsilon_{33}^{eff} \end{bmatrix} \begin{bmatrix} \bar{S}_{11} \\ \bar{S}_{22} \\ \bar{S}_{33} \\ \bar{S}_{23} \\ \bar{S}_{31} \\ \bar{S}_{12} \\ \bar{E}_1 \\ \bar{E}_2 \\ \bar{E}_3 \end{bmatrix} \tag{57}$$

In addition, the constants are provided in matrix form, adhering to the IEEE format. In this format, the tensor indices are expressed using matrix or Voigt notation, following the scheme: $11 \rightarrow 1$; $22 \rightarrow 2$; $33 \rightarrow 3$; $23 = 32 \rightarrow 4$; $13 = 31 \rightarrow 5$; $12 = 21 \rightarrow 6$. For example, a tensor constant C_{1123} is expressed as C_{14} in Voigt notation.

Eq. (57) introduces a 9×9 matrix that represents the general variables involved in the coupled electromechanical problem. However, in the case of the homogenised structure, these variables are replaced with their respective values. Specifically, the effective material coefficients are denoted as C_{ij}^{eff}, d_{ij}^{eff} and ε_{ij}^{eff}, while the average values are represented by $\bar{T}_{ij}$, $\bar{D}_i$, $\bar{S}_{ij}$ and $\bar{E}_i$. These relationships serve as the basis for further considerations based on RVE.

4.5.1. Boundary condition implementation approach

To determine the effective coefficients, specific boundary conditions are applied to the RVE. The objective was to isolate one component of the strain/electric field vector in Eq. (57) while setting all other components to zero. This controlled setup enables the straightforward calculation of each effective coefficient by multiplying the corresponding row of the material matrix by the strain/electric field vector. To achieve this, appropriate boundary conditions and constraint equations were applied to different surfaces of the RVE, as shown in Fig. 8. Table 4 provides a comprehensive overview of the necessary boundary conditions for calculating all effective coefficients [53,54,95,98,126,134]. Additionally, the Table 4 includes the final formulas extracted from Eq. (57) for each specific configuration.

In the Table 4, specific notation is used to describe the various applied boundary condition configurations, ensuring clarity in understanding the different setups used for evaluating the effective coefficients. Through this systematic approach and the utilisation of Table 4, the study enables precise determination of the effective coefficients, which play a vital role in characterising the RVE's response to strain and electric fields.

4.5.2. Energy-based approach

The energy-based approach has proven to be a valuable method for assessing the effective modulus and dielectric constant of piezoelectric composites, as highlighted in [54,170]. In this method, the elastic strain energy (U_e), dielectric energy (U_d), and electromechanical energy (U_{em}) within a piezoelectric composite was analysed, as described by Eq. (58), (59) and (60). To determine the overall energies of RVEs, the energies of each RVE element were summed. Here, V represents the volume of the RVE, while C_{ijkl}^{eff} and ε_{ij}^{eff} denote the effective elastic modulus and dielectric tensor, respectively. Additionally, S_{ij}^{eff} and E_i^{eff} stand for the strain and electric field tensors applied to the RVE. The strain and electric field tensors applied to the RVE are determined by applying the mechanical displacement and electrical potential boundary conditions, as shown in Table 4. This energy-based approach has also been effectively employed to ascertain the effective electroelastic properties of piezoelectric structural fibre composites, as demonstrated in [125,126].

This comprehensive method allows us to gain a deep understanding of the composite materials' behaviour, taking into account both mechanical and electrical aspects.

$$U_e = \sum_{m=1}^{n} U_e^m = \frac{V}{2} C_{ijkl}^{eff} S_{ij}^{eff} S_{kl}^{eff} \tag{58}$$

$$U_d = \sum_{m=1}^{n} U_d^m = \frac{V}{2} \varepsilon_{ij}^{eff} E_i^{eff} E_j^{eff} \tag{59}$$

$$U_{em} = \sum_{m=1}^{n} U_{em}^m = \frac{V}{2} d_{ijk}^{eff} S_{ij}^{eff} E_i^{eff} \tag{60}$$

4.6. Optimisation of electro-mechanical behaviour

Optimisation of electro-mechanical behaviour refers to the process of improving the performance and efficiency of composites that involve both electrical and mechanical components. Optimising these composites requires a deep understanding of both domains and finding ways to seamlessly integrate them for improved overall performance. Choosing the right materials for both electrical and mechanical components is also crucial. Materials should possess properties that enhance the composite's performance, such as conductivity for electrical components or strength and durability for mechanical parts. The design of electro-mechanical composites plays a critical role in their optimisation. So, it is needed to consider factors like the arrangement of components, the size and shape of parts, and the overall layout to ensure optimal performance. The optimisation of electro-mechanical behaviour is a multidisciplinary field that seeks to improve the performance, efficiency, and safety of systems that combine electrical and mechanical elements. It requires a holistic approach, from material selection and design to control systems and environmental considerations, and it plays a pivotal role in advancing technology across various industries.

Topology optimisation is a powerful technique that helps determine the ideal layout or arrangement of a structure or material while adhering to specific design constraints. It can be enhanced by integrating homogenisation, which enables the creation of intricate RVE shapes. This combination expands the range of achievable material properties, going beyond the typical fibre-reinforced or laminate materials [171–173]. These novel materials can also be engineered to exhibit unconventional characteristics.

Furthermore, in the realm of topology optimisation, it is possible to manipulate the polarisation direction of piezoelectric materials as a design variable [174]. In finite element analysis, the orientation of local polarisation within each element is described as an angle relative to a fixed reference point. Consequently, the design variables can take on continuous values within predefined limits. However, there is a drawback to this approach: it leads to a non-convex global solution space, which introduces challenges related to multiple local minima [175].

To tackle this issue, the Discrete Material Optimization (DMO) method has been introduced. This method combines gradient-based techniques with mathematical programming to address discrete optimisation problems [92]. Its creators, Stegmann et al. [175], initially applied it to solve problems related to the orientation of orthotropic materials and material selection. It is also applicable to situations that involve both aspects, such as the optimisation of general composite laminate shell structures. Notably, the DMO method can be employed to optimise the local polarisation directions of piezoelectric materials at individual points, serving as an effective strategy for handling the complexities associated with multiple local minima problems. Topology optimisation involves a crucial concept known as the adaptive design domain [176]. This domain is essentially a predefined, fixed region that must encompass the entire structure under consideration during the optimisation process. The main objective here is to determine where material should be added or removed within this fixed domain to create

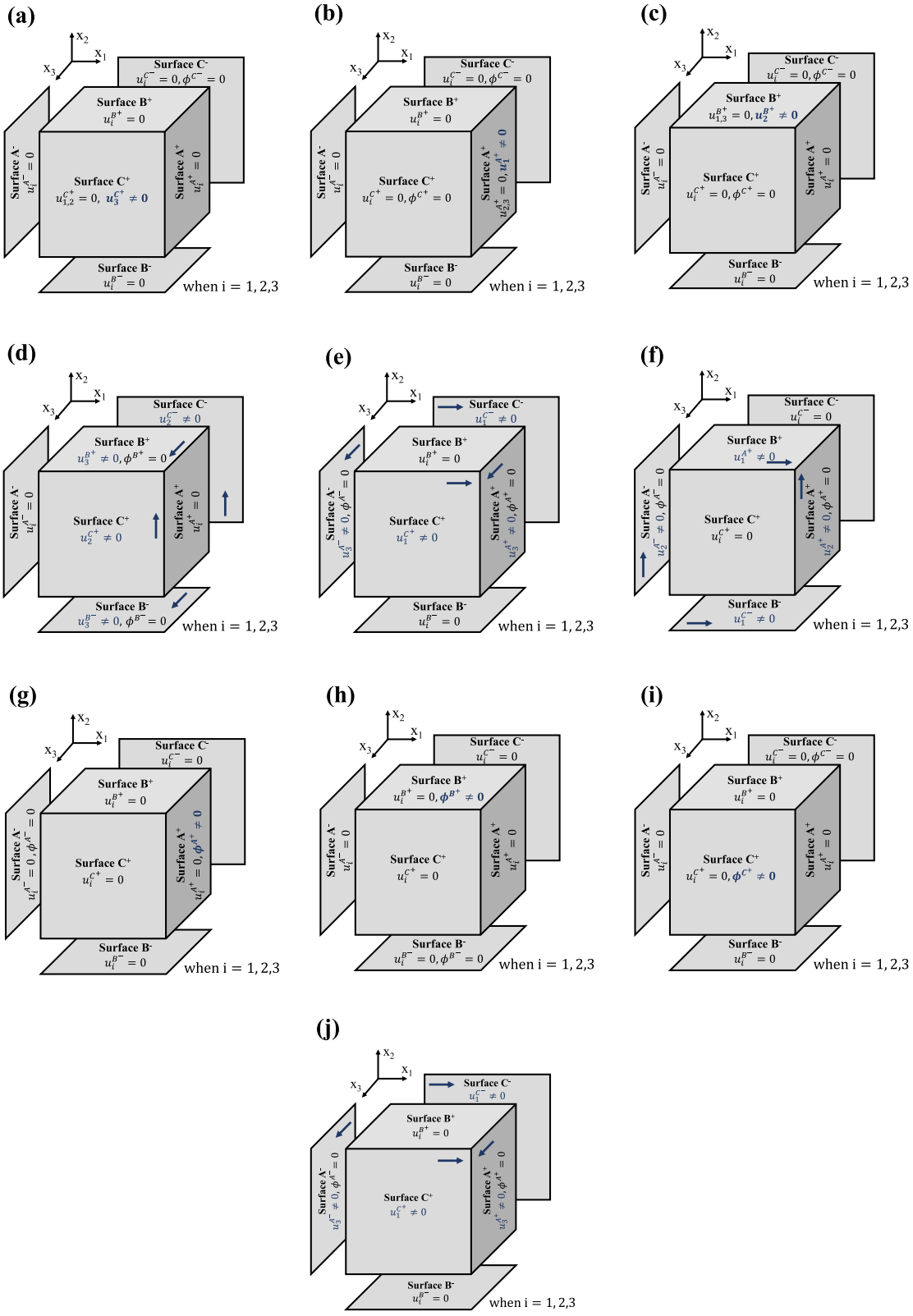

Fig. 8. Periodic boundary condition to calculate the effective coefficients (a) $\mathbf{C}_{13}^{\mathbf{eff}}$, $\mathbf{C}_{23}^{\mathbf{eff}}$ and $\mathbf{C}_{33}^{\mathbf{eff}}$; (b) $\mathbf{C}_{11}^{\mathbf{eff}}$ and $\mathbf{C}_{12}^{\mathbf{eff}}$; (c) $\mathbf{C}_{22}^{\mathbf{eff}}$; (d) $\mathbf{C}_{44}^{\mathbf{eff}}$; (e) $\mathbf{C}_{55}^{\mathbf{eff}}$; (f) $\mathbf{C}_{66}^{\mathbf{eff}}$; (g) $\varepsilon_{11}^{\mathbf{eff}}$; (h) $\varepsilon_{22}^{\mathbf{eff}}$; (i) $\varepsilon_{33}^{\mathbf{eff}}$; (j) $\mathbf{d}_{13}^{\mathbf{eff}}$ and $\mathbf{d}_{33}^{\mathbf{eff}}$.

Table 4
Summary of boundary conditions and equations for calculation of the effective coefficients [53,54,95,98,126,134].

Eff. Coeff.	$A^-(x)$ (u_i/Φ)	$A^+(x)$ (u_i/Φ)	$B^-(y)$ (u_i/Φ)	$B^+(y)$ (u_i/Φ)	$C^-(z)$ (u_i/Φ)	$C^+(z)$ (u_i/Φ)	Equation
C_{11}^{eff}	0/-	$\tilde{u}_1$/-	0/-	0/-	0/0	0/0	$\bar{T}_{11}/\bar{S}_{11}$
C_{12}^{eff}	0/-	$\tilde{u}_1$/-	0/-	0/-	0/0	0/0	$\bar{T}_{22}/\bar{S}_{11}$
C_{22}^{eff}	0/-	0/-	0/-	$\tilde{u}_2$/-	0/0	0/0	$\bar{T}_{22}/\bar{S}_{22}$
C_{13}^{eff}	0/-	0/-	0/-	0/-	0/0	$\tilde{u}_3$/-	$\bar{T}_{11}/\bar{S}_{33}$
C_{23}^{eff}	0/-	0/-	0/-	0/-	0/0	$\tilde{u}_3$/-	$\bar{T}_{22}/\bar{S}_{33}$
C_{33}^{eff}	0/-	0/-	0/-	0/-	0/0	$\tilde{u}_3$/-	$\bar{T}_{33}/\bar{S}_{33}$
C_{44}^{eff}	0/-	0/-	$(\tilde{u}_3)$/0	$(\tilde{u}_3)$/0	$(\tilde{u}_2)$/-	$(\tilde{u}_2)$/-	$\bar{T}_{23}/\bar{S}_{23}$
C_{55}^{eff}	$(\tilde{u}_3)$/0	$(\tilde{u}_3)$/0	0/-	0/-	$(\tilde{u}_1)$/-	$(\tilde{u}_1)$/-	$\bar{T}_{31}/\bar{S}_{31}$
C_{66}^{eff}	$(\tilde{u}_2)$/-	$(\tilde{u}_2)$/-	$(\tilde{u}_1)$/-	$(\tilde{u}_1)$/-	0/0	0/0	$\bar{T}_{12}/\bar{S}_{12}$
d_{13}^{eff}	0/-	0/-	0/-	0/-	0/0	$0/\tilde{\Phi}$	$-\bar{T}_{11}/\bar{E}_3$
d_{15}^{eff}	$(\tilde{u}_3)$/0	$(\tilde{u}_3)$/0	0/-	0/-	$(\tilde{u}_1)$/-	$(\tilde{u}_1)$/-	$\bar{D}_1/\bar{S}_{31}$
d_{33}^{eff}	0/-	0/-	0/-	0/-	0/0	$0/\tilde{\Phi}$	$-\bar{T}_{33}/\bar{E}_3$
ϵ_{11}^{eff}	0/0	$0/\tilde{\Phi}$	0/-	0/-	0/-	0/-	$\bar{D}_1/\bar{E}_1$
ϵ_{22}^{eff}	0/-	0/-	0/0	$0/\tilde{\Phi}$	0/-	0/-	$\bar{D}_2/\bar{E}_2$
ϵ_{33}^{eff}	0/-	0/-	0/-	0/-	0/0	$0/\tilde{\Phi}$	$\bar{D}_3/\bar{E}_3$

Legend:.
0 denotes a prescribed zero displacement or electric potential.
- denotes a non-prescribed electric potential.
$\tilde{u}_i$ denotes a non-zero prescribed displacement for the component u_i.
$\tilde{\Phi}$ denotes a non-zero prescribed electric potential Φ.
$(\tilde{u}_i)$ denotes a constraint of coupling with the opposite surface for displacement component u_i, as shown in Fig. 7b.

the desired structure, including holes and connections. Importantly, this fixed nature of the adaptive domain means that the underlying finite element model remains unchanged throughout the optimisation process. This stability simplifies the calculation of derivatives for functions defined over this adaptive domain [177,178]. In the context of material design, this adaptive design domain typically corresponds to the RVE domain. This is where the optimisation procedure operates.

In Fig. 9 is presented how topology optimisation is applied to the design of piezocomposite materials. Initially, a mesh is generated within the predefined domain, and the optimisation process is conducted. This process results in a topology or layout, which can then be further refined, verified, and eventually manufactured.

The discrete nature of the problem presents a challenge. In this case, each element can only have a material value of either zero (phase 1 or void) or one (phase 2 or solid material). This binary constraint makes it a challenging and ill-posed problem. To address this, a common approach is to relax the problem by allowing materials to assume intermediate values during the optimisation process. This relaxation is achieved by defining a specialised material model. Essentially, this material model approximates the material distribution by using a continuous parameter (a design variable) to determine the mixture of basic materials throughout the domain. In doing so, the relaxation transforms the problem into a continuous material design problem, eliminating the need for clear-cut connectivity between materials [179–181].

A topology solution can be obtained by applying penalisation coefficients to the material model. These coefficients help recover the binary 0–1 design (indicating void or solid materials) and enable a discernible connectivity. Some control mechanisms for material distribution, such as filters or projections, are also employed to ensure the smoothness of the material layout [182].

It is important to note that this relaxed problem bears a strong resemblance to the problem of Functionally Graded Material (FGM) design. FGM design seeks a continuous transition of material properties within a structure. Consequently, while the 0–1 design problem requires complexity control, such as using filters, to avoid intermediate values of design variables, the FGM design problem allows for solutions with intermediate material property values. This flexibility is a distinguishing feature between these two approaches [92,183].

4.7. Summary

In recent years, the field of piezoelectric materials and composites has seen significant advancements, thanks to the application of Finite Element Analysis (FEA) and various modelling techniques. These techniques have enabled researchers to gain a deeper understanding of the electromechanical properties of piezoelectric materials, leading to improved designs and applications. Numerous studies have contributed to this progress. For instance, Odegard et al. [54] introduced a novel FEA model that enhanced the accuracy of predictions regarding piezoelectric composite properties. Meanwhile, Mishra et al. [134] employed 3D FEM models with periodic boundaries to analyse electroelastic nanocomposites, with a specific focus on PMN-0.3PT/PDMS nanocomposites. The results from these studies offer valuable insights into the behaviour of these materials.

Additionally, studies like [159,160] used FEA to investigate the acoustic properties and porosity effects on piezoelectric materials, respectively. These studies not only provided theoretical insights but also validated their models against experimental data, enhancing the credibility of their findings. Furthermore, research such as [94,126] delved into the optimisation of electromechanical behaviour and the analysis of piezoelectric fibre composites, utilising FEA alongside analytical and numerical approaches. These interdisciplinary approaches have enabled a comprehensive understanding of the materials' properties and behaviour.

In the context of nanocomposites, some studies [78,79] explored the impacts of surface piezoelectricity and introduced an extended Mori-Tanaka method to model size-dependent moduli accurately. These developments are crucial for designing nanocomposite materials with specific properties. Moreover, studies like [101,133] highlighted the optimisation of piezoelectric transducers and energy harvesters using FEA and genetic algorithms. These optimisation techniques play a vital role in enhancing the efficiency and performance of piezoelectric devices.

In summary, the application of FEA and various modelling techniques in the study of piezoelectric materials and composites has significantly advanced our understanding of their properties and behaviour. These studies, despite in Table 5, demonstrate the importance of computational methods in driving innovation and progress in

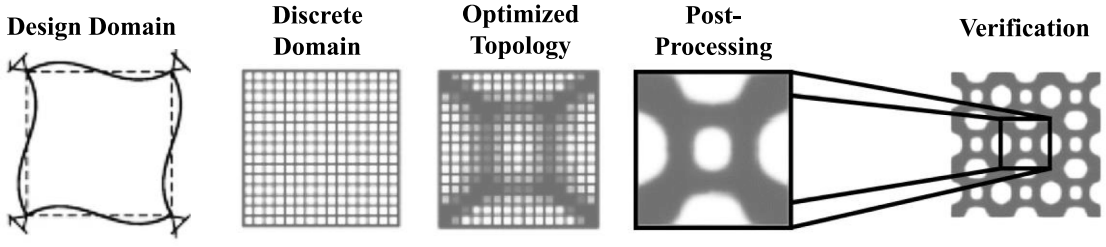

Fig. 9. Design steps for topology optimisation of the piezocomposite materials (based on [92]).

Table 5
Overview of the numeric models developed to study piezoelectric composites.

Type of piezoelectric composites	Ref.	Material behaviour	Electro-mechanical behaviour	Validation (analytical models)	Software used	RVE element type/ mesh	Focus of study	Main conclusions
Particulate composites	[54] (2004)	A	Linear	MTA SCA	ANSYS	Tetrahedral elements. **SOLID98:** 10 nodes/elem; 4 DOF/node (3 displacements and 1 V. RVE hexagonal packing; C_p=0.6.	Novel model predicts piezoelectric composite properties, compared with Mori-Tanaka and FEA.	Novel model predicts piezoelectric composite properties with greater accuracy. The comparison shows the model's agreement with finite element analysis.
	[134] (2023)	A	Linear	MTA SCA	ABAQUS through Python interface	Tetrahedral elements. **C3D4E:** 4 nodes/ elem; 4 DOF/node (3 displacements and 1 V). 100 × 100 × 100 nm; element size of 6 nm.	3D FEM model with periodic boundaries analyses electroelastic 0–3 nanocomposites.	Periodic-boundary FEM determines the properties of PMN-0.3PT/PDMS nanocomposite, considering reinforcement effects. FEM matches Eshelby/Mori – Tanaka model at low reinforcement fractions; interphase is crucial.
Porous within Composites	[160] (2005)	A	Linear	Experimental Data	ANSYS	–	FEM studies the acoustic properties of dense and porous piezoceramic hydrophones.	Models match experimental results, aiding 3–3 piezocomposite transducer design. Porous piezocomposites suitable for broad-frequency hydrophone applications were confirmed experimentally.
	[161] (2006)	TI	Linear	ETM	ABAQUS	Hexahedral elements. **C3D8E:** 8 nodes/ elem; 4 DOF/node (3 displacements and 1 V). Hexahedral elements.	The FEM model assesses porosity effects on piezoelectric material properties.	The study comprehends 3–1-type porous piezoelectric material electromechanical behaviour. RVE FE model captures properties, and porosity influence, and enhances material utility.
	[162] (2007)	TI	Linear	ETM	ABAQUS	Hexahedral elements. **C3D8E:** 8 nodes/ elem; 4 DOF/node (3 displacements and 1 V).	The FEM model quantifies porosity distribution impact on transversely porous.	Porosity geometry strongly influences piezoelectric material properties. Porosity distribution affects figures of merit like acoustic impedance.
	[20] (2011)	A	Linear	MBM	ABAQUS	**C3D8E:** 8 nodes/ elem; 4 DOF/node (3 displacements and 1 V). Square arrangement.	The FEM model predicts electromechanical properties of various porous piezoelectric.	The study investigates optimising 3–0 type porous piezoelectric materials' properties. 3–0 type flat-cuboidal porosity enhances hydrophone performance significantly.
	[104] (2020)	TI	Linear	AHBM	FreeFEM++	Tetrahedral elements.	AHM-FEM coupling computes effective properties of porous thermo-piezoelectric composites for energy harvesting.	FEM is applied directly to AHM local problems for accurate solutions. The homogenised model agrees well with, the potential for nonlinear extensions.
	[90] (2022)	A	Linear	–	ANSYS	Tetrahedral elements. **SOLID227:** 10 nodes/elem; 4 DOF/node (3 displacements and 1 V. SHELL281/ TARGE170. Elements size: L/8 and L/10.	Metal-layered porous piezoelectric composite with improved interfacial properties explored.	Metal-coated porous piezoelectric composite enhances properties, impacting stiffness and efficiency. Optimal constituent fractions for diverse applications in actuators and sensing.
Long-fiber Composites	[132] (1999)	TI	Linear	ETM DAA MTA SCA	ABAQUS	**C3D20E:** 20 nodes/ elem; 4 DOF/node (3 displacements and 1 V).	Study models 1–3 and 0–3 piezoceramic composites for effective piezoelectric constants.	Effective piezoelectric constants were derived numerically and compared with analytical data.

(*continued on next page*)

Table 5 (*continued*)

Type of piezoelectric composites	Ref.	Material behaviour	Electro-mechanical behaviour	Validation (analytical models)	Software used	RVE element type/ mesh	Focus of study	Main conclusions
						Meshes with 1000 elements for accurate 0–3 composite analysis.		RVE methods balance the advantages of analytical and FE analysis.
	[190] (2000)	TI	Linear	–	ABAQUS	Hexagonal and square arrangements; C_f=0.4.	FE RVE model simulates diverse deformation modes in fibre composites.	Extensive FE RVE model analyses periodic fibre composites' behaviour. The model captures overall and local properties and considers various loading.
	[54] (2004)	A	Linear	MTA SCA	ANSYS	Tetrahedral elements. **SOLID98:** 10 nodes/elem; 4 DOF/node (3 displacements and 1 V. RVE hexagonal packing; C_f=0.9	Novel model predicts piezoelectric composite properties, compared with Mori-Tanaka and FEA.	Novel model predicts piezoelectric composite properties with greater accuracy. The comparison shows the model's agreement with finite element analysis.
	[96] (2005)	A	Linear	AHBM	ANSYS FORTRAN	8 nodes/elem; 4 DOF/node (3 displacements and 1 V). Square arrangement.	Numerical FEM predicts effective coefficients of piezoelectric fibre composites.	Numerical FEM predicts piezoelectric fibre composite properties accurately. Developed tool interfaces ANSYS and FORTRAN for efficient calculations.
	[191] (2007)	TI	Linear	–	ABAQUS	**C3D8E:** 8 nodes/ elem; 4 DOF/node (3 displacements and 1 V). Rectangular and square-shaped RVEs.	Numerical FEM model assesses fibre distribution effects in active composites.	The numerical FEM model investigates the effects of fibre distribution in piezoelectric composites. Longitudinal properties linear, transverse non-linear; figures of merit consistent.
	[99] (2007)	TI	Linear	–	ANSYS	Tetrahedral elements. **SOLID98:** 10 nodes/elem; 4 DOF/node (3 displacements and 1 V.	The method uses FEM and RVE for effective properties evaluation in randomly distributed piezoelectric composites.	Numerical techniques reveal volume fraction's dominant role in effective properties. The generalised ANSYS-based method automates evaluation for diverse fibre composites.
	[125] (2011)	TI	Linear	MTA	ANSYS	**PLANE223:** 8 nodes/elem; 3 DOF/node (2 displacements and 1 V).	Optimise the electromechanical behaviour of 0–3 composites.	The paper presents an FE-based approach for predicting piezoelectric composites' properties. Mori-Tanaka approximation suits elastic, dielectric properties; FEM captures piezoelectric response.
	[94] (2011)	A	Linear	MBM	ABAQUS	**C3D8E:** 8 nodes/ elem; 4 DOF/node (3 displacements and 1 V). Mesh with 1000 elements.	Development of a homogenised model for orthotropic behaviour of MFCs.	Analytical and numerical approaches yield consistent results for composite properties. Matrix mechanical properties affect piezoelectric behaviour in transducers.
	[126] (2012)	TI	Linear	MTA	ABAQUS	**C3D20E:** 20 nodes/ elem; 4 DOF/node (3 displacements and 1 V). C_f=0.4; 5 mm length in the longitudinal direction.	Examine the electromechanical properties via micromechanics and FEM of piezoelectric fibre composites.	Piezoelectric structural fibre (PSF) composites enhance piezoelectric material durability via the core-coating technique. Micromechanics and FE analysis predict electro-elastic PSF properties effectively.
	[75] (2013)	TI	Linear	MTA	ABAQUS	**C3D20E:** 20 nodes/ elem; 4 DOF/node (3 displacements and 1 V).	Multi-Inclusion model predicts electroelastic properties in multiphase piezoelectric composites.	Multifunctional materials benefit from functionally graded interfaces for enhanced properties. Extended Multi-Inclusion model predicts electroelastic properties

(*continued on next page*)

Table 5 (*continued*)

Type of piezoelectric composites	Ref.	Material behaviour	Electro-mechanical behaviour	Validation (analytical models)	Software used	RVE element type/ mesh	Focus of study	Main conclusions
								accurately with low computational cost.
	[106] (2014)	TI	Linear	AHBM	ABAQUS	**C3D20E:** 20 nodes/ elem; 4 DOF/node (3 displacements and 1 V).	Effective properties computed via FEA, RVE, and asymptotic homogenization for active fibre composites.	Numerical results align well with analytical and semi-analytical approaches. Numerical accuracy and validation through experimental tests are essential.
	[52] (2020)	TI	Linear	MBM	ABAQUS	**C3D8E:** 8 nodes/ elem; 4 DOF/node (3 displacements and 1 V).	Models predict effective properties of hollow fibre-reinforced piezocomposites.	Excellent agreement of predicted properties with finite-element analysis. Modified models predict enhanced properties of hollow-fibre reinforced composites.
	[53] (2022)	TI	Linear	MBM MTA	ANSYS APDL	Tetrahedral elements. **SOLID226/ SOLID186:** 20 nodes/elem; 4 DOF/node (3 displacements and 1 V.	MBM predicts coefficients for transverse-loaded piezoelectric composites via FEM validation.	Novel analytical model captures fibre arrangement impact in piezoelectric composites. FEM validation shows fibre packing affects elastic, piezoelectric coefficients significantly.
	[79] (2022)	TI	Linear	ETM	*	48 × 12 Quadratic quadrilateral elements. Hexagonal RVE.	Demonstrating classical models' efficacy in predicting piezoelectric nanocomposite properties.	Novel methods analyse surface piezoelectricity impact on nanoporous materials. Accurate models are established; caution is required for negative surface energy interfaces.
	[78] (2023)	TI	Linear	ETM	*	48 × 12 Quadratic quadrilateral elements. Hexagonal RVE.	Innovative extended Mori-Tanaka method explores piezoelectric behaviour in nanoporous composites.	Novel extended Mori-Tanaka method models piezoelectric nanocomposites with surface effects. The analytical approach predicts size-dependent moduli, opening inelasticity extension possibilities.
Periodic Grid	[192] (2012)	A	Linear	–	ABAQUS	**C3D8E:** 8 nodes/ elem; 4 DOF/node (3 displacements and 1 V). Porosity volume fractions = 0.7 – 1; Foam structures.	3D FEM model analyses piezoelectric foam properties and interconnect influence.	A comprehensive study explores the electro-mechanical properties of porous piezoelectric foams. The finite element model characterises diverse foam structures for improved applications.
Laminate Composites	[101] (2016)	TI	Linear	AHBM	ABAQUS	**C3D8E:** 8 nodes/ elem; 4 DOF/node (3 displacements and 1 V).	Design of a multilayered piezoelectric transducer based on a special RVE homogenization method	AHBM and genetic algorithm optimise unidirectional piezoelectric transducers. Optimal design yields directional dependency with enhanced performance.
	[133] (2017)	A	Linear (AHBM)	–	ANSYS	Cubic elements. **SOLID226:** 4 nodes/elem; 4 DOF/node (3 displacements and 1 V). 14 × 14 × 14 cm (0.025 cm/elem).	Optimise the harvester power output of the unimorph vibration harvester configuration.	Introduced and validated the model's accuracy and used it to optimise energy harvesters. Found that adjusting material orientation, circuit resistance, and composite properties boost power output and efficiency.
	[193] (2022)	I	Nonlinear	–	COMSOL	–	Proposal of linear-arc composite beam for enhanced piezoelectric energy harvesting.	Linear-arc composite beam PEH—C was designed and analysed through simulation and experiment. Curvature affects resonance, stress, and open-circuit voltage output performance.

(*continued on next page*)

Table 5 (*continued*)

Type of piezoelectric composites	Ref.	Material behaviour	Electro-mechanical behaviour	Validation (analytical models)	Software used	RVE element type/ mesh	Focus of study	Main conclusions
	[194] (2022)	A	Nonlinear	–	*	Isoparametric elements. 8 nodes/elem. 100 elements.	The finite element model analyses smart composite plates with distributed piezoelectric materials.	Efficient FE model developed for analysing smart composite plates. The model was successfully applied to study static, dynamic, and control behaviour.
FGPBs	[152] (2002)	TI	Linear	Modified Lamination Theory	ANSYS	15 000 elements	Evaluate the deflection characteristics of the bimorph actuator with FGPBs.	An FGPB PZT/Pt piezoelectric bimorph actuator shows enhanced deflection performance and stress distribution compared to non-graded bimorphs. Utilising modified lamination theory, the linear profile minimises stress and maintains bimorph bending.
	[159] (2015)	A	Nonlinear (MBM)	Experimental Data	*	A unit is divided into 8 subcells, representing the inclusion and matrix.	Analysis of nonlinear responses in functionally graded piezoelectric beams.	Multi-scale model analyses nonlinear responses of functionally graded beams. Electric fields induce bending and polarization switching in actuators.

Legend: FGPBs – functionally graded piezoelectric beams; TI – transversely isotropic; A – anisotropic; LDT – Landau–Devanshire theory; MBM – micromechanics-based models; ETM – Eshelby-type models; DAA – dilute approximation approach; MTA – Mori–Tanaka approach; SCA – self-consistent approach; AHBM – asymptotic homogenization-based model; $C_{f \text{ or } p}$ – fiber or particle volume fraction; * - undefined.

this field, paving the way for exciting future developments in piezoelectric technology. Numerical homogenisation techniques typically depend on the FEA. However, a notable drawback of these methods is the necessity for meshing, which becomes laborious as the complexity of the microstructure increases. To address this challenge, a recent approach based on Fourier transforms has been employed for analysing composite materials with coupled local laws [184]. Initially introduced for evaluating the response of elastic-type composites [185], this alternative method has since been utilised to explore the effective behaviour and distribution of local mechanical fields across a diverse range of behaviours and microstructures [186,187] This computational technique harnesses a rapid Fourier transform algorithm, allowing for the utilisation of microstructure images in computations without the need for meshing.

Additionally, there are alternative numerical methodologies that can be employed to analyse the behaviour of piezoelectric composites. The finite-volume approach has emerged as a firmly established technique within the numerical engineering realm, facilitating the simulation of diverse challenges in fluid dynamics and solid mechanics. Nevertheless, its adoption within the heterogeneous media mechanics community has been sluggish, frequently entangled with misconceptions related to the finite-element method or purported higher-order theories. This approach holds the capability to address boundary-value problems in solid mechanics, with recent advancements focusing on resolving unit cell dilemmas in periodic heterogeneous media [188,189].

5. Conclusion

This paper offers a comprehensive review of research endeavours dedicated to analytically and numerically modelling RVEs, encompassing aspects like spatial fibre distribution generation, constitutive modelling, and the application of periodic boundary conditions. In the course of our exploration, several key findings and noteworthy insights have come to the fore.

A prominent focus emerges on long-fibre composites that exhibit either transversely isotropic or anisotropic properties. This emphasis can be attributed to the inherent limitations of Eshelby-Type Models in accurately predicting the effective transverse modulus. Eshelby-type models have their niche utility, particularly in scenarios involving specific reinforcement shapes. However, they grapple with limitations related to interactions, laminate considerations, and predictions of transverse modulus.

On the other hand, Micromechanics-Based Models offer simplicity and directional predictability but struggle when it comes to transverse properties, often yielding results dominated by the matrix phase. Moreover, they tend to encounter challenges when dealing with materials exhibiting high anisotropy. For those studying composites involving particles or porous structures, Micromechanics-Based Models and Asymptotic Homogenization-Based Models have gained prominence. The latter proves efficient for unravelling the complexities of microstructures but is more effective when these structures conform to regular patterns. Highly contrasting materials can pose challenges for Asymptotic Homogenization-Based Models.

It is important to note that only a limited number of numerical models have been experimentally validated. Furthermore, the realm of numerical modelling for metallic matrices remains relatively uncharted.

In conclusion, this review underscores the diverse landscape of modelling strategies for RVEs, with each approach exhibiting its strengths and limitations. Researchers in this field must carefully select the appropriate modelling technique based on the specific characteristics of their composite materials and the desired level of accuracy. Additionally, there is a pressing need for further experimental validation of numerical models, particularly in the context of metallic matrices, to enhance the reliability and applicability of these modelling techniques in real-world scenarios.

CRediT authorship contribution statement

Pedro M. Ferreira: Writing – original draft, Visualization, Methodology, Investigation, Formal analysis, Data curation. **Miguel A. Machado:** Writing – review & editing, Methodology, Formal analysis. **Catarina Vidal:** Writing – review & editing, Supervision, Resources, Project administration, Methodology, Funding acquisition, Formal analysis, Conceptualization. **Marta S. Carvalho:** Writing – review &

editing, Methodology, Formal analysis, Conceptualization.

Declaration of competing interest

The authors declare that they have no known competing financial interests or personal relationships that could have appeared to influence the work reported in this paper.

Data availability

No data was used for the research described in the article.

Acknowledgements

PMF also acknowledges FCT - Fundação para a Ciência e a Tecnologia for funding the PhD grant UI/BD/151055/2021. PMF, MAM, CV and MSC acknowledge FCT - Fundação para a Ciência e a Tecnologia for its financial support via projects UIDB/00667/2020 and UIDP/00667/2020 (UNIDEMI).

References

[1] Sony S, Laventure S, Sadhu A. A literature review of next-generation smart sensing technology in structural health monitoring. Struct Control Heal Monit 2019;26:e2321. https://doi.org/10.1002/stc.2321.
[2] Ferreira PM, Machado MA, Carvalho MS, Vidal C. Embedded sensors for structural health monitoring: methodologies and applications review. Sensors 2022;22. https://doi.org/10.3390/s22218320.
[3] Das Mahapatra S, PC Mohapatra, Aria AI, Christie G, Mishra YK, Hofmann S, et al. Piezoelectric materials for energy harvesting and sensing applications: roadmap for future smart materials. Adv Sci 2021;8:2100864. https://doi.org/10.1002/advs.202100864.
[4] Eltouby P, Shyha I, Li C, Khaliq J. Factors affecting the piezoelectric performance of ceramic-polymer composites: a comprehensive review. Ceram Int 2021;47:17813–25. https://doi.org/10.1016/j.ceramint.2021.03.126.
[5] Mokhtari F, Azimi B, Salehi M, Hashemikia S, Danti S. Recent advances of polymer-based piezoelectric composites for biomedical applications. J Mech Behav Biomed Mater 2021;122. https://doi.org/10.1016/j.jmbbm.2021.104669.
[6] Stuber VL, Deutz DB, Bennett J, Cannel D, de Leeuw DM, van der Zwaag S, et al. Flexible lead-free piezoelectric composite materials for energy harvesting applications. Energy Technol 2019;7:177–85. https://doi.org/10.1002/ente.201800419.
[7] Wang Z, Maruyama K, Narita F. A novel manufacturing method and structural design of functionally graded piezoelectric composites for energy-harvesting. Mater Des 2022;214. https://doi.org/10.1016/j.matdes.2021.110371.
[8] Rendas P, Figueiredo L, Machado C, Mourão A, Vidal C, Soares B. Mechanical performance and bioactivation of 3D-printed PEEK for high-performance implant manufacture: a review. Prog Biomater 2023;12:89–111. https://doi.org/10.1007/s40204-022-00214-6.
[9] Rendas P, Figueiredo L, Cláudio R, Vidal C, Soares B. Investigating the effects of printing temperatures and deposition on the compressive properties and density of 3D printed polyetheretherketone. Prog Addit Manuf 2023. https://doi.org/10.1007/s40964-023-00550-4.
[10] Wu J. Perovskite lead-free piezoelectric ceramics. J Appl Phys 2020;127:190901. https://doi.org/10.1063/5.0006261.
[11] Guo Q, Li F, Xia F, Wang P, Gao X, Hao H, et al. Piezoelectric ceramics with high piezoelectricity and broad temperature usage range. J Mater 2021;7:683–92. https://doi.org/10.1016/j.jmat.2020.11.012.
[12] Ferreira PM, Machado MA, Carvalho MS, Vidal C. Granting sensorial properties to metal parts through friction stir processing. Meas J Int Meas Confed 2023;207. https://doi.org/10.1016/j.measurement.2022.112405.
[13] Ferreira PM, Machado MA, Carvalho MS, Vidal C. Self-sensing metallic material based on piezoelectric particles. Res Rev J Nondestruct Test 2023;1. https://doi.org/10.58286/28107.
[14] Zheng T, Wu J. Origin of large piezoelectricity in BF-BT based multiphase ferroelectrics. Ceram Int 2022;48:23808–13. https://doi.org/10.1016/j.ceramint.2022.05.035.
[15] Liu C, Xu P, Zheng D, Liu Q. Study on microstructure and properties of a Fe-based SMA/PZT composite coating produced by laser cladding. J Alloys Compd 2020;831:154813. https://doi.org/10.1016/j.jallcom.2020.154813.
[16] Ferreira PM, Machado MA, Carvalho MS, Vilaça P, Sorger G, Pinto JV, et al. Self-sensing metallic material based on PZT particles produced by friction stir processing envisaging structural health monitoring applications. Mater Charact 2023;205:113371. https://doi.org/10.1016/j.matchar.2023.113371.
[17] Vidal C, Ferreira PM, Inácio PL, Ferreira FB, Santiago D, Meneses P, et al. Particles' distribution enhancing in aluminum-based composites produced by upward friction stir processing. Int J Adv Manuf Technol 2023;127:2745–57. https://doi.org/10.1007/s00170-023-11664-y.
[18] Moreira F, Ferreira PM, Silva RJC, Santos TG, Vidal C. Aluminium-based dissimilar alloys surface composites reinforced with functional microparticles produced by upward friction stir processing. Coatings 2023;13. https://doi.org/10.3390/coatings13050962.
[19] Habib M, Lantgios I, Hornbostel K. A review of ceramic, polymer and composite piezoelectric materials. J Phys D Appl Phys 2022;55. https://doi.org/10.1088/1361-6463/ac8687.
[20] Iyer S, Venkatesh TA. Electromechanical response of (3-0) porous piezoelectric materials: effects of porosity shape. J Appl Phys 2011;110. https://doi.org/10.1063/1.3622509.
[21] Wei C, Jing X. A comprehensive review on vibration energy harvesting: modelling and realization. Renew Sustain Energy Rev 2017;74:1–18. https://doi.org/10.1016/j.rser.2017.01.073.
[22] Mishra S, Unnikrishnan L, Nayak SK, Mohanty S. Advances in piezoelectric polymer composites for energy harvesting applications: a systematic review. Macromol Mater Eng 2019;304:1800463. https://doi.org/10.1002/mame.201800463.
[23] Liu H, Lin X, Zhang S, Huan Y, Huang S, Cheng X. Enhanced performance of piezoelectric composite nanogenerator based on gradient porous PZT ceramic structure for energy harvesting. J Mater Chem A 2020;8:19631–40. https://doi.org/10.1039/D0TA03054F.
[24] Hailu B, Hayward G, Gachagan A, McNab A, Farlow R. Comparison of different piezoelectric materials for the design of embedded transducers for structural health monitoring applications. Proc IEEE Ultrason Symp 2000;2:1009–13. https://doi.org/10.1109/ultsym.2000.921495.
[25] Sakamoto WK, Higuti RT, Crivelini EB, Nagashima HN. Polymer matrix-based piezoelectric composite for structural health monitoring. In: 2013 Jt IEEE Int Symp Appl Ferroelectr Work Piezoresponse Force Microsc ISAF/PFM 2013; 2013. p. 295–7. https://doi.org/10.1109/ISAF.2013.6748696.
[26] Nguyen VC, Le MQ, Fimbel A, Bernadet S, Hebrard Y, Mogniotte JF, et al. Printing smart coating of piezoelectric composite for application in condition monitoring of bearings. Mater Des 2022;215. https://doi.org/10.1016/j.matdes.2022.110529.
[27] Grinberg D, Siddique S, Le MQ, Liang R, Capsal JF, Cottinet PJ. 4D Printing based piezoelectric composite for medical applications. J Polym Sci Part B Polym Phys 2019;57:109–15. https://doi.org/10.1002/polb.24763.
[28] Ding W, Liu Y, Shiotani T, Wang Q, Han N, Xing F. Cement-based piezoelectric ceramic composites for sensing elements: a comprehensive state-of-the-art review. Sensors 2021;21. https://doi.org/10.3390/s21093230.
[29] Santos D, Machado MA, Monteiro J, Sousa JP, Proença CS, Crivellaro FS, et al. Non-destructive inspection of high temperature piping combining ultrasound and eddy current testing. Sensors 2023;23:3348. https://doi.org/10.3390/s23063348.
[30] Silva HV, Catapirra NP, Carvalho MS, Santos TG, Machado MA. Nondestructive testing of 3D printed fiber-reinforced polymeric composites: an experimental critical comparison. 3D Print Addit Manuf 2023. https://doi.org/10.1089/3dp.2022.0291.
[31] Machado MA, Rosado LS, Santos TG. Shaping eddy currents for non-destructive testing using additive manufactured magnetic substrates. J Nondestruct Eval 2022;41:50. https://doi.org/10.1007/s10921-022-00882-1.
[32] Guedes J, Kikuchi N. Preprocessing and postprocessing for materials based on the homogenization method with adaptive finite element methods. Comput Method Appl Mech Eng 1990;83:143–98. https://doi.org/10.1016/0045-7825(90)90148-F.
[33] Shedbale AS, Singh IV, Mishra BK. Heterogeneous and homogenized models for predicting the indentation response of particle reinforced metal matrix composites. Int J Mech Mater Des 2017;13:531–52. https://doi.org/10.1007/s10999-016-9352-3.
[34] American National Standard. IEEE standard of piezoelectricity. New York; 1987.
[35] Uchino K. Advanced piezoelectric materials: science and technology. 2nd ed. Woodhead Publishing; 2010. https://doi.org/10.1533/9781845699758.
[36] Nelli Silva ECEC, Ono Fonseca JS, Kikuchi N. Optimal design of periodic piezocomposites. Comput Method Appl Mech Eng 1998;159:49–77. https://doi.org/10.1016/S0045-7825(98)80103-5.
[37] Hashimoto KY, Yarnaguchi M. Elastic, piezoelectric and dielectric properties of composite materials. In: IEEE 1986 Ultrason. Symp. IEEE; 1986. p. 697–702. https://doi.org/10.1109/ULTSYM.1986.198824.
[38] Banno H. Effects of shape and volume fraction of closed pores on remanent polarization and coercive force of ferroelectric ceramics. Jpn J Appl Phys 1987;26:50. https://doi.org/10.7567/JJAPS.26S2.50.
[39] Adnan Islam R, Priya S. Progress in dual (piezoelectric-magnetostrictive) phase magnetoelectric sintered composites. Adv Condens Matter Phys 2012;2012:1–29. https://doi.org/10.1155/2012/320612.
[40] Levassort F, Lethiecq M, Millar C, Pourcelot L. Modeling of highly loaded 0-3 piezoelectric composites using a matrix method. IEEE Trans Ultrason Ferroelectr Freq Control 1998;45:1497–505. https://doi.org/10.1109/58.738289.
[41] Levassort F, Lethiecq M, Certon D, Patat F. A matrix method for modeling electroelastic moduli of 0-3 piezo-composites. IEEE Trans Ultrason Ferroelectr Freq Control 1997;44:445–52. https://doi.org/10.1109/58.585129.
[42] Levassort F, Lethiecq M, Desmare R. Effective electroelastic moduli of 3-3(0-3) piezocomposites. IEEE Trans Ultrason Ferroelectr Freq Control 1999;46:1028–34. https://doi.org/10.1109/58.775670.
[43] Kim J-Y. Effective elastic constants of anisotropic multilayers. Mech Res Commun 2001;28:97–101. https://doi.org/10.1016/S0093-6413(01)00149-5.

[44] Wang X, Pan E, Albrecht JD, Feng WJ. Effective properties of multilayered functionally graded multiferroic composites. Compos Struct 2009;87:206–14. https://doi.org/10.1016/j.compstruct.2008.01.006.
[45] Topolov VY, Krivoruchko AV. Polarization orientation effect and combination of electromechanical properties in advanced 0.67Pb(Mg 1/3 Nb 2/3)O 3 –0.33PbTiO 3 single crystal/polymer composites with 2–2 connectivity. Smart Mater Struct 2009;18:065011. https://doi.org/10.1088/0964-1726/18/6/065011.
[46] Bowen CR, Topolov VY. Piezoelectric sensitivity of PbTiO3-based ceramic/polymer composites with 0–3 and 3–3 connectivity. Acta Mater 2003;51:4965–76. https://doi.org/10.1016/S1359-6454(03)00283-0.
[47] Kar-Gupta R, Venkatesh TA. Electromechanical response of 1–3 piezoelectric composites: an analytical model. Acta Mater 2007;55:1093–108. https://doi.org/10.1016/j.actamat.2006.09.023.
[48] Kar-Gupta R, Venkatesh TA. Electromechanical response of (2–2) layered piezoelectric composites. Smart Mater Struct 2013;22:025035. https://doi.org/10.1088/0964-1726/22/2/025035.
[49] Tan P, Tong L. Micro-electromechanics models for piezoelectric-fiber-reinforced composite materials. Compos Sci Technol 2001;61:759–69. https://doi.org/10.1016/S0266-3538(01)00014-8.
[50] Mallik N, Ray MC. Effective Coefficients of Piezoelectric Fiber-Reinforced Composites. AIAA J 2003;41:704–10. https://doi.org/10.2514/2.2001.
[51] Kumar A, Chakraborty D. Effective properties of thermo-electro-mechanically coupled piezoelectric fiber reinforced composites. Mater Des 2009;30:1216–22. https://doi.org/10.1016/j.matdes.2008.06.009.
[52] Aimmanee S, Asanuma H. Micromechanics-based predictions of effective properties of a 1-3 piezocomposite reinforced with hollow piezoelectric fibers. Mech Adv Mater Struct 2020;27:1873–87. https://doi.org/10.1080/15376494.2018.1529842.
[53] Singh SK, Panda SK. A comparative study of micromechanics models to evaluate effective coefficients of 1-3 piezoelectric composite. Mech Adv Mater Struct 2022:1–14. https://doi.org/10.1080/15376494.2022.2092799.
[54] Odegard GM. Constitutive modeling of piezoelectric polymer composites. Acta Mater 2004;52:5315–30. https://doi.org/10.1016/j.actamat.2004.07.037.
[55] Dinzart F, Sabar H. Electroelastic behavior of piezoelectric composites with coated reinforcements: micromechanical approach and applications. Int J Solids Struct 2009;46:3556–64. https://doi.org/10.1016/j.ijsolstr.2009.05.019.
[56] Eshelby John Douglas. The determination of the elastic field of an ellipsoidal inclusion, and related problems. Proc R Soc London Ser A Math Phys Sci 1957;241:376–96. https://doi.org/10.1098/rspa.1957.0133.
[57] Kinoshita N, Mura T. Elastic fields of inclusions in anisotropic media. Phys Status Solidi 1971;5:759–68. https://doi.org/10.1002/pssa.2210050332.
[58] Walpole LJ. The elastic field of an inclusion in an anisotropic medium. Proc R Soc London Ser A Math Phys Sci 1967;300:270–89. https://doi.org/10.1098/rspa.1967.0170.
[59] Gavazzi AC, Lagoudas DC. On the numerical evaluation of Eshelby's tensor and its application to elastoplastic fibrous composites. Comput Mech 1990;7:13–9. https://doi.org/10.1007/BF00370053.
[60] Biao W. Three-dimensional analysis of an ellipsoidal inclusion in a piezoelectric material. Int J Solid Struct 1992;29:293–308. https://doi.org/10.1016/0020-7683(92)90201-4.
[61] Benveniste Y. The determination of the elastic and electric fields in a piezoelectric inhomogeneity. J Appl Phys 1992;72:1086–95. https://doi.org/10.1063/1.351784.
[62] Dunn ML, Taya M. Micromechanics predictions of the effective electroelastic moduli of piezoelectric composites. Int J Solid Struct 1993;30:161–75. https://doi.org/10.1016/0020-7683(93)90058-F.
[63] Chen T. An invariant treatment of interfacial discontinuities in piezoelectric media. Int J Eng Sci 1993;31:1061–72. https://doi.org/10.1016/0020-7225(93)90114-A.
[64] Mikata Y. Determination of piezoelectric Eshelby tensor in transversely isotropic piezoelectric solids. Int J Eng Sci 2000;38:605–41. https://doi.org/10.1016/S0020-7225(99)00050-6.
[65] Deeg WFJ. The analysis of dislocation, crack, and inclusion problems in piezoelectric solids. Stanford University; 1980.
[66] Dunn ML, Taya M. An analysis of piezoelectric composite materials containing ellipsoidal inhomogeneities. Proc R Soc London Ser A Math Phys Sci 1993;443:265–87. https://doi.org/10.1098/rspa.1993.0145.
[67] Chen T. Green's functions and the non-uniform transformation problem in a piezo electric medium. Mech Res Commun 1993;20:271–8. https://doi.org/10.1016/0093-6413(93)90069-Z.
[68] Dunn ML, Taya M. Electromechanical properties of porous piezoelectric ceramics. J Am Ceram Soc 1993;76:1697–706. https://doi.org/10.1111/j.1151-2916.1993.tb06637.x.
[69] Dunn ML, Wienecke H. Inclusions and inhomogeneities in transversely isotropic piezoelectric solids. Int J Solid Struct 1997;34:3571–82. https://doi.org/10.1016/S0020-7683(96)00209-0.
[70] Mikata Y. Explicit determination of piezoelectric Eshelby tensors for a spheroidal inclusion. Int J Solid Struct 2001;38:7045–63. https://doi.org/10.1016/S0020-7683(00)00419-4.
[71] Fakri N, Azrar L, El Bakkali L. Electroelastic behavior modeling of piezoelectric composite materials containing spatially oriented reinforcements. Int J Solid Struct 2003;40:361–84. https://doi.org/10.1016/S0020-7683(02)00524-3.
[72] Chen Z, Yu S, Meng L, Lin Y. Effective properties of layered magneto-electro-elastic composites. Compos Struct 2002;57:177–82. https://doi.org/10.1016/S0263-8223(02)00081-8.
[73] Hori M, Nemat-Nasser S. Universal bounds for effective piezoelectric moduli. Mech Mater 1998;30:1–19. https://doi.org/10.1016/S0167-6636(98)00029-5.
[74] Mori T, Tanaka K. Average stress in matrix and average elastic energy of materials with misfitting inclusions. Acta Metall 1973;21:571–4. https://doi.org/10.1016/0001-6160(73)90064-3.
[75] Malakooti MH, Sodano HA. Multi-Inclusion modeling of multiphase piezoelectric composites. Compos Part B Eng 2013;47:181–9. https://doi.org/10.1016/j.compositesb.2012.10.034.
[76] Rodríguez-Ramos R, Otero JA, Espinosa-Almeyda Y, Sabina FJ, Levin V. Closed-form expressions for the effective properties of piezoelastic composites reinforced with cylindrical fibers by Maxwell scheme. Mech Mater 2022;174. https://doi.org/10.1016/j.mechmat.2022.104452.
[77] Hasanzadeh M, Ansari R, Hassanzadeh-Aghdam MK. Evaluation of effective properties of piezoelectric hybrid composites containing carbon nanotubes. Mech Mater 2019;129:63–79. https://doi.org/10.1016/j.mechmat.2018.11.003.
[78] Chen Q, Chatzigeorgiou G, Meraghni F. Extended mean-field homogenization of unidirectional piezoelectric nanocomposites with generalized Gurtin-Murdoch interfaces. Compos Struct 2023;307. https://doi.org/10.1016/j.compstruct.2022.116639.
[79] Chen Q, Chatzigeorgiou G, Meraghni F, Javili A. Homogenization of size-dependent multiphysics behavior of nanostructured piezoelectric composites with energetic surfaces. Eur J Mech A/Solid 2022;96. https://doi.org/10.1016/j.euromechsol.2022.104731.
[80] Rodríguez-Ramos R, Gandarilla-Pérez CA, Lau-Alfonso L, Lebon F, Sabina FJ, Sevostianov I. Maxwell homogenization scheme for piezoelectric composites with arbitrarily-oriented spheroidal inhomogeneities. Acta Mech 2019;230:3613–32. https://doi.org/10.1007/s00707-019-02481-0.
[81] Hori M, Nemat-Nasser S. Double-inclusion model and overall moduli of multi-phase composites. Mech Mater 1993;14:189–206. https://doi.org/10.1016/0167-6636(93)90066-Z.
[82] Hershey AV. The elasticity of an isotropic aggregate of anisotropic cubic crystals. J Appl Mech 1954;21:236–40. https://doi.org/10.1115/1.4010899.
[83] Kröner E. Berechnung der elastischen Konstanten des Vielkristalls aus den Konstanten des Einkristalls. Zeitschrift Für Phys 1958;151:504–18. https://doi.org/10.1007/BF01337948.
[84] Jacquet E, Trivaudey F, Varchon D. Calculation of the transverse modulus of a unidirectional composite material and of the modulus of an aggregate. Application of the rule of mixtures. Compos Sci Technol 2000;60:345–50. https://doi.org/10.1016/S0266-3538(99)00128-1.
[85] Gałka A, Telega JJ, Wojnar R. Homogenization and thermopiezoelectricity. Mech Res Commun 1992;19:315–24. https://doi.org/10.1016/0093-6413(92)90050-K.
[86] Sigmund O, Torquato S, Aksay IA. On the design of 1–3 piezocomposites using topology optimization. J Mater Res 1998;13:1038–48. https://doi.org/10.1557/JMR.1998.0145.
[87] Challagulla KS, Venkatesh TA. Electromechanical response of 2-2 layered piezoelectric composites: a micromechanical model based on the asymptotic homogenization method. Philos Mag 2009;89:1197–222. https://doi.org/10.1080/14786430902915412.
[88] Bravo-Castillero J, Guinovart-Díaz R, Sabina FJ, Rodríguez-Ramos R. Closed-form expressions for the effective coefficients of a fiber-reinforced composite with transversely isotropic constituents - II. Piezoelectric and square symmetry. Mech Mater 2001;33:237–48. https://doi.org/10.1016/S0167-6636(00)00060-0.
[89] Bisegna P, Luciano R. On methods for bounding the overall properties of periodic piezoelectric fibrous composites. J Mech Phys Solids 1997;45:1329–56. https://doi.org/10.1016/S0022-5096(96)00116-0.
[90] Nasedkin A, Nassar ME. A numerical study about the effects of the metal volume fraction on the effective properties of a porous piezoelectric composite with metalized pore boundaries. Mech Adv Mater Struct 2022;29:4359–72. https://doi.org/10.1080/15376494.2021.1928346.
[91] Georgiades AV, Kalamkarov AL, Challagulla KS. Asymptotic homogenization model for generally orthotropic reinforcing networks in smart composite plates. Smart Mater Struct 2006;15:1197–210. https://doi.org/10.1088/0964-1726/15/5/006.
[92] Vatanabe SL, Paulino GH, Silva ECN. Design of functionally graded piezocomposites using topology optimization and homogenization - Toward effective energy harvesting materials. Comput Method Appl Mech Eng 2013;266:205–18. https://doi.org/10.1016/j.cma.2013.07.003.
[93] Li-Kun W, Li L, Lei Q, Weiwei W, Tianxiao D. Study of effective properties of modified 1-3 piezocomposites. J Appl Phys 2008;104. https://doi.org/10.1063/1.2975343.
[94] Nasser H, Biscani F, Belouettar S. Effect of matrix properties on the overall piezoelectric constants of piezocomposite transducers. Mech Adv Mater Struct 2011;18:531–9. https://doi.org/10.1080/15376494.2011.605011.
[95] Berger H, Kari S, Gabbert U, Rodriguez-Ramos R, Guinovart R, Otero JA, et al. An analytical and numerical approach for calculating effective material coefficients of piezoelectric fiber composites. Int J Solids Struct 2005;42:5692–714. https://doi.org/10.1016/j.ijsolstr.2005.03.016.
[96] Berger H, Kari S, Gabbert U, Rodríguez-Ramos R, Bravo-Castillero J, Guinovart-Díaz R. A comprehensive numerical homogenisation technique for calculating effective coefficients of uniaxial piezoelectric fibre composites. Mater Sci Eng A 2005;412:53–60. https://doi.org/10.1016/j.msea.2005.08.035.
[97] Berger H, Kari S, Gabbert U, Rodriguez-Ramos R, Bravo-Castillero J, Guinovart-Diaz R. Calculation of effective coefficients for piezoelectric fiber composites based on a general numerical homogenization technique. Compos Struct 2005;71:397–400. https://doi.org/10.1016/j.compstruct.2005.09.038.

[98] Berger H, Kari S, Gabbert U, Rodriguez-Ramos R, Bravo-Castillero J, Guinovart-Diaz R, et al. Unit cell models of piezoelectric fiber composites for numerical and analytical calculation of effective properties. Smart Mater Struct 2006;15:451–8. https://doi.org/10.1088/0964-1726/15/2/026.

[99] Kari S, Berger H, Rodriguez-Ramos R, Gabbert U. Numerical evaluation of effective material properties of transversely randomly distributed unidirectional piezoelectric fiber composites. J Intell Mater Syst Struct 2007;18:361–72. https://doi.org/10.1177/1045389X06066293.

[100] Iyer S, Venkatesh TA. Electromechanical response of (3–0,3–1) particulate, fibrous, and porous piezoelectric composites with anisotropic constituents: a model based on the homogenization method. Int J Solid Struct 2014;51:1221–34. https://doi.org/10.1016/j.ijsolstr.2013.12.008.

[101] Nasser H, Porn S, Koutsawa Y, Giunta G, Belouettar S. Optimal design of a multilayered piezoelectric transducer based on a special unit cell homogenization method. Acta Mech 2016;227:1837–47. https://doi.org/10.1007/s00707-016-1581-x.

[102] Qin QH. Material properties of piezoelectric composites by BEM and homogenization method. Compos Struct 2004;66:295–9. https://doi.org/10.1016/j.compstruct.2004.04.051.

[103] Reda H, Karathanasopoulos N, Maurice G, Ganghoffer JF, Lakiss H. Computation of effective piezoelectric properties of stratified composites and application to wave propagation analysis. ZAMM Zeitschrift Fur Angew Math Und Mech 2020;100. https://doi.org/10.1002/zamm.201900251.

[104] Caballero-Pérez RO, Bravo-Castillero J, Pérez-Fernández LD, Rodríguez-Ramos R, Sabina FJ. Computation of effective thermo-piezoelectric properties of porous ceramics via asymptotic homogenization and finite element methods for energy-harvesting applications. Arch Appl Mech 2020;90:1415–29. https://doi.org/10.1007/s00419-020-01675-6.

[105] Nasimsobhan M, Ganghoffer JF, Shamshirsaz M. Construction of piezoelectric and flexoelectric models of composites by asymptotic homogenization and application to laminates. Math Mech Solids 2022;27:602–37. https://doi.org/10.1177/10812865211030317.

[106] De Medeiros R, Rodríguez-Ramos R, Guinovart-Díaz R, Bravo-Castillero J, Otero JA, Tita V. Numerical and analytical analyses for active fiber composite piezoelectric composite materials. J Intell Mater Syst Struct 2015;26:101–18. https://doi.org/10.1177/1045389X14521881.

[107] Hanse Wampo FL, Ntenga R, Effa JY, Lapusta Y, Ntamack GE, Maréchal P. Generalized homogenization model of piezoelectric materials for ultrasonic transducer applications. J Compos Mater 2022;56:713–26. https://doi.org/10.1177/00219983211058806.

[108] Gerasimenko TE, Kurbatova NV, Nadolin DK, Nasedkin AV, Nasedkina AA, Oganesyan PA, et al. Homogenization of piezoelectric composites with internal structure and inhomogeneous polarization in ACELAN-COMPOS finite element package. Adv Struct Mater 2019;109:113–31. https://doi.org/10.1007/978-3-030-17470-5_8.

[109] Nasedkin AV, Nasedkina AA, Nassar ME. Homogenization of porous piezocomposites with extreme properties at pore boundaries by effective moduli method. Mech Solid 2020;55:827–36. https://doi.org/10.3103/S0025654420050131.

[110] Camarena E, Yu W. Improved analytical homogenization of the piezoelectric macro-fiber composite: active layer embedded among passive layers. Smart Mater Struct 2019;28. https://doi.org/10.1088/1361-665X/ab0b60.

[111] Challagulla S, Unnikrishna Pillai A, Rahaman MM. A novel homogenization method for periodic piezoelectric composites via diffused material interface. Mech Adv Mater Struct 2023:1–20. https://doi.org/10.1080/15376494.2023.2219112.

[112] Agrawal A, Prakash V, Rahaman MM. A diffused material interface based homogenization method for periodic composites. Mech Adv Mater Struct 2022;29:5979–92. https://doi.org/10.1080/15376494.2021.1970865.

[113] Hassan EM, Kalamkarov AL, Georgiades AV, Challagulla KS. An asymptotic homogenization model for smart 3D grid-reinforced composite structures with generally orthotropic constituents. Smart Mater Struct 2009;18:075006. https://doi.org/10.1088/0964-1726/18/7/075006.

[114] Challagulla KS, Georgiades AV, Kalamkarov AL. Asymptotic homogenization modeling of smart composite generally orthotropic grid-reinforced shells: part I – theory. Eur J Mech - A/Solid 2010;29:530–40. https://doi.org/10.1016/j.euromechsol.2010.03.007.

[115] Georgiades AV, Challagulla KS, Kalamkarov AL. Asymptotic homogenization modeling of smart composite generally orthotropic grid-reinforced shells: part II–Applications. Eur J Mech - A/Solid 2010;29:541–56. https://doi.org/10.1016/j.euromechsol.2010.03.006.

[116] Kalamkarov AL, Savi MA. Micromechanical modeling and effective properties of the smart grid-reinforced composites. J Braz Soc Mech Sci Eng 2012;34:343–51. https://doi.org/10.1590/S1678-58782012000500002.

[117] Saha GC, Kalamkarov AL, Georgiades AV. Micromechanical analysis of effective piezoelastic properties of smart composite sandwich shells made of generally orthotropic materials. Smart Mater Struct 2007;16:866–83. https://doi.org/10.1088/0964-1726/16/3/037.

[118] Jayachandran KP, Guedes JM, Rodrigues HC. Stochastic optimization of ferroelectric ceramics for piezoelectric applications. Struct Multidiscip Optim 2011;44:199–212. https://doi.org/10.1007/s00158-011-0626-y.

[119] Jayachandran KP, Guedes JM, Rodrigues HC. Homogenization of textured as well as randomly oriented ferroelectric polycrystals. Comput Mater Sci 2009;45:816–20. https://doi.org/10.1016/j.commatsci.2008.05.027.

[120] Mawassy N, Reda H, Ganghoffer JF, Lakiss H. Control of the piezoelectric and flexoelectric homogenized properties of architected materials by tuning their inner topology. Mech Res Commun 2023;127. https://doi.org/10.1016/j.mechrescom.2022.104034.

[121] Dunn ML. Electroelastic Green's functions for transversely isotropic piezoelectric media and their application to the solution of inclusion and inhomogeneity problems. Int J Eng Sci 1994;32:119–31. https://doi.org/10.1016/0020-7225(94)90154-6.

[122] Dunn ML, Wienecke HA. Green's functions for transversely isotropic piezoelectric solids. Int J Solid Struct 1996;33:4571–81. https://doi.org/10.1016/0020-7683(95)00282-0.

[123] Wang B. Effective behavior of piezoelectric composites. Appl Mech Rev 1994;47:S112–21. https://doi.org/10.1115/1.3122806.

[124] Chen T. Effective properties of platelet reinforced piezocomposites. Compos Part B Eng 1996;27:467–74. https://doi.org/10.1016/1359-8368(96)00014-5.

[125] Chambion B, Goujon L, Badie L, Mugnier Y, Barthod C, Galez C, et al. Optimization of the piezoelectric response of 0–3 composites: a modeling approach. Smart Mater Struct 2011;20:115006. https://doi.org/10.1088/0964-1726/20/11/115006.

[126] Dai Q, Ng K. Investigation of electromechanical properties of piezoelectric structural fiber composites with micromechanics analysis and finite element modeling. Mech Mater 2012;53:29–46. https://doi.org/10.1016/j.mechmat.2012.04.014.

[127] Lee CK. Theory of laminated piezoelectric plates for the design of distributed sensors/actuators. Part I: governing equations and reciprocal relationships. J Acoust Soc Am 1990;87:1144–58. https://doi.org/10.1121/1.398788.

[128] Trzepieciński T, Ryzińska G, Gromada M, Biglar M. 3D microstructure-based modelling of the deformation behaviour of ceramic matrix composites. J Eur Ceram Soc 2018;38:2911–9. https://doi.org/10.1016/j.jeurceramsoc.2017.11.038.

[129] Rodríguez-Ramos R, Sabina FJ, Guinovart-Díaz R, Bravo-Castillero J. Closed-form expressions for the effective coefficients of a fiber-reinforced composite with transversely isotropic constituents – I. Elastic and square symmetry. Mech Mater 2001;33:223–35. https://doi.org/10.1016/S0167-6636(00)00059-4.

[130] Otero JA, Rodríguez-Ramos R, Monsivais G, Pérez-Alvarez R. Dynamical behavior of a layered piezocomposite using the asymptotic homogenization method. Mech Mater 2005;37:33–44. https://doi.org/10.1016/j.mechmat.2003.12.004.

[131] Hashin Z. Analysis of composite materials—a survey. J Appl Mech 1983;50:481–505. https://doi.org/10.1115/1.3167081.

[132] Poizat C, Sester M. Effective properties of composites with embedded piezoelectric fibres. Comput Mater Sci 1999;16:89–97. https://doi.org/10.1016/S0927-0256(99)00050-6.

[133] Matos AM, Guedes JM, Jayachandran KP, Rodrigues HC. Computational model for power optimization of piezoelectric vibration energy harvesters with material homogenization. Comput Struct 2017;192:144–56. https://doi.org/10.1016/j.compstruc.2017.07.015.

[134] Mishra N, Das K. A finite element study of interphase properties and reinforcement size effect on the electro-elastic properties of PMN-0.3PT/PDMS nanocomposite. Mater Today Commun 2023;34. https://doi.org/10.1016/j.mtcomm.2022.105308.

[135] Tressler JF, Alkoy S, Newnham RE. Piezoelectric sensors and sensor materials. J Electroceramics 1998;2:257–72. https://doi.org/10.1023/A:1009926623551.

[136] Takahashi J. An introduction to the theory of piezoelectricity, 11; 1960. https://doi.org/10.4057/jsr.11.2_51.

[137] Hauke T, Kouvatov A, Steinhausen R, Seifert W, Beige H, Langhammer HT, et al. Bending behavior of functionally gradient materials. Ferroelectrics 2000;238:195–202. https://doi.org/10.1080/00150190008008784.

[138] Wang BL, Noda N. Design of a smart functionally graded thermopiezoelectric composite structure. Smart Mater Struct 2001;10:189–93. https://doi.org/10.1088/0964-1726/10/2/303.

[139] Bhangale RK, Ganesan N. Static analysis of simply supported functionally graded and layered magneto-electro-elastic plates. Int J Solid Struct 2006;43:3230–53. https://doi.org/10.1016/j.ijsolstr.2005.05.030.

[140] Carbonari RC, Silva ECN, Paulino GH. Multi-actuated functionally graded piezoelectric micro-tools design: a multiphysics topology optimization approach. Int J Numer Method Eng 2009;77:301–36. https://doi.org/10.1002/nme.2403.

[141] Carbonari RC, Silva ECN, Paulino GH. Topology optimization design of functionally graded bimorph-type piezoelectric actuators. Smart Mater Struct 2007;16:2605–20. https://doi.org/10.1088/0964-1726/16/6/065.

[142] Ladvanjari D, Mahajan A, Dhanjode A, Patil RK. Static and modal analysis of functionally graded piezoelectric plate for sensor responses. Mater Today Proc 2023;72:1678–84. https://doi.org/10.1016/j.matpr.2022.09.468.

[143] Vatanabe SL, Paulino GH, Silva ECN. Influence of pattern gradation on the design of piezocomposite energy harvesting devices using topology optimization. Compos Part B Eng 2012;43:2646–54. https://doi.org/10.1016/j.compositesb.2012.03.023.

[144] Bhangale RK, Ganesan N. Free vibration of simply supported functionally graded and layered magneto-electro-elastic plates by finite element method. J Sound Vib 2006;294:1016–38. https://doi.org/10.1016/j.jsv.2005.12.030.

[145] Huang DJ, Ding HJ, Chen WQ. Analysis of functionally graded and laminated piezoelectric cantilever actuators subjected to constant voltage. Smart Mater Struct 2008;17. https://doi.org/10.1088/0964-1726/17/6/065002.

[146] Panda S, Ray MC. Geometrically nonlinear analysis of smart functionally graded plates integrated with a layer of vertically reinforced 1-3 piezoelectric composite. Acta Mech 2008;198:235–51. https://doi.org/10.1007/s00707-007-0529-6.

[147] Yang YZ. Analysis of elasticity solution of Bi-direction functionally graded piezoelectric beam subject to voltage. Appl Mech Mater 2012;166–169:824–7. https://doi.org/10.4028/www.scientific.net/AMM.166-169.824.

[148] Pramanik R, Arockiarajan A. Effective properties and nonlinearities in 1-3 piezocomposites: a comprehensive review. Smart Mater Struct 2019;28:103001. https://doi.org/10.1088/1361-665X/ab350a.
[149] Tiersten HF. Electroelastic equations for electroded thin plates subject to large driving voltages. J Appl Phys 1993;74:3389–93. https://doi.org/10.1063/1.354565.
[150] Kouvatov A, Steinhausen R, Hauke T, Langhammer HT, Beige H, Abicht H. Poling behavior of functionally gradient material bending devices. Ferroelectrics 2002;273:95–100. https://doi.org/10.1080/00150190211759.
[151] Jin D, Meng Z. Functionally graded PZT/ZnO piezoelectric composites. J Mater Sci Lett 2003;22:971–4. https://doi.org/10.1023/A:1024612929936.
[152] Takagi K, Li J-F, Yokoyama S, Watanabe R, Almajid A, Taya M. Design and fabrication of functionally graded PZT/Pt piezoelectric bimorph actuator. Sci Technol Adv Mater 2002;3:217–24. https://doi.org/10.1016/S1468-6996(02)00017-7.
[153] Lin CH, Muliana A. Micromechanical models for the effective time-dependent and nonlinear electromechanical responses of piezoelectric composites. J Intell Mater Syst Struct 2014;25:1306–22. https://doi.org/10.1177/1045389X13504477.
[154] Lin CH, Muliana A. Micromechanics models for the effective nonlinear electro-mechanical responses of piezoelectric composites. Acta Mech 2013;224:1471–92. https://doi.org/10.1007/s00707-013-0823-4.
[155] Muliana AH. A micromechanical formulation for piezoelectric fiber composites with nonlinear and viscoelastic constituents. Acta Mater 2010;58:3332–44. https://doi.org/10.1016/j.actamat.2010.02.007.
[156] Aboudi J. Hysteresis behavior of ferroelectric fiber composites. Smart Mater Struct 2005;14:715–26. https://doi.org/10.1088/0964-1726/14/4/030.
[157] Aboudi J. Micromechanical prediction of the effective coefficients of thermo-piezoelectric multiphase composites. J Intell Mater Syst Struct 1998;9:713–22. https://doi.org/10.1177/1045389X9800900903.
[158] Newnham RE, Bowen LJ, Klicker KA, Cross LE. Composite piezoelectric transducers. Mater Des 1980;2:93–106. https://doi.org/10.1016/0261-3069(80)90019-9.
[159] Lin C-H, Muliana A. Nonlinear electro-mechanical responses of functionally graded piezoelectric beams. Compos Part B Eng 2015;72:53–64. https://doi.org/10.1016/j.compositesb.2014.11.030.
[160] Ramesh R, Kara H, Bowen CR. Finite element modelling of dense and porous piezoceramic disc hydrophones. Ultrasonics 2005;43:173–81. https://doi.org/10.1016/j.ultras.2004.05.001.
[161] Kar-Gupta R, Venkatesh TA. Electromechanical response of porous piezoelectric materials. Acta Mater 2006;54:4063–78. https://doi.org/10.1016/j.actamat.2006.04.037.
[162] Kar-Gupta R, Venkatesh TA. Electromechanical response of porous piezoelectric materials: effects of porosity distribution. Appl Phys Lett 2007;91. https://doi.org/10.1063/1.2766960.
[163] Coelho PG, Amiano LD, Guedes JM, Rodrigues HC. Scale-size effects analysis of optimal periodic material microstructures designed by the inverse homogenization method. Comput Struct 2016;174:21–32. https://doi.org/10.1016/j.compstruc.2015.10.001.
[164] Saraev D, Schmauder S. Finite element modelling of Al/SiCp metal matrix composites with particles aligned in stripes—A 2D–3D comparison. Int J Plast 2003;19:733–47. https://doi.org/10.1016/S0749-6419(01)00058-4.
[165] Zhang J, Ouyang Q, Guo Q, Li Z, Fan G, Su Y, et al. 3D Microstructure-based finite element modeling of deformation and fracture of SiCp/Al composites. Compos Sci Technol 2016;123:1–9. https://doi.org/10.1016/j.compscitech.2015.11.014.
[166] Ciomaga CE, Horchidan N, Padurariu L, Stirbu RS, Tiron V, Tufescu FM, et al. $BaTiO_3$ nanocubes-Gelatin composites for piezoelectric harvesting: modeling and experimental study. Ceram Int 2022;48:25880–93. https://doi.org/10.1016/j.ceramint.2022.05.264.
[167] Tian W, Qi L, Chao X, Liang J, Fu M. Periodic boundary condition and its numerical implementation algorithm for the evaluation of effective mechanical properties of the composites with complicated micro-structures. Compos Part B Eng 2019;162:1–10. https://doi.org/10.1016/j.compositesb.2018.10.053.
[168] Sun CT, Vaidya RS. Prediction of composite properties from a representative volume element. Compos Sci Technol 1996;56:171–9. https://doi.org/10.1016/0266-3538(95)00141-7.
[169] Damjanovic D. Ferroelectric, dielectric and piezoelectric properties of ferroelectric thin films and ceramics. Reports Prog Phys 1998;61:1267–324. https://doi.org/10.1088/0034-4885/61/9/002.
[170] Lin Y, Sodano HA. A double inclusion model for multiphase piezoelectric composites. Smart Mater Struct 2010;19:035003. https://doi.org/10.1088/0964-1726/19/3/035003.
[171] Sigmund O, Torquato S. Design of materials with extreme thermal expansion using a three-phase topology optimization method. J Mech Phys Solids 1997;45:1037–67. https://doi.org/10.1016/S0022-5096(96)00114-7.
[172] Sigmund O. Tailoring materials with prescribed elastic properties. Mech Mater 1995;20:351–68. https://doi.org/10.1016/0167-6636(94)00069-7.
[173] Sigmund O. Materials with prescribed constitutive parameters: an inverse homogenization problem. Int J Solids Struct 1994;31:2313–29. https://doi.org/10.1016/0020-7683(94)90154-6.
[174] Rupp CJ, Evgrafov A, Maute K, Dunn ML. Design of piezoelectric energy harvesting systems: a topology optimization approach based on multilayer plates and shells. J Intell Mater Syst Struct 2009;20:1923–39. https://doi.org/10.1177/1045389X09341200.
[175] Stegmann J, Lund E. Discrete material optimization of general composite shell structures. Int J Numer Methods Eng 2005;62:2009–27. https://doi.org/10.1002/nme.1259.
[176] Rong Y, Zhao Z-L, Feng X-Q, Xie YM. Structural topology optimization with an adaptive design domain. Comput Methods Appl Mech Eng 2022;389:114382. https://doi.org/10.1016/j.cma.2021.114382.
[177] Allaire G, Bonnetier E, Francfort G, Jouve F. Shape optimization by the homogenization method. Numer Math 1997;76:27–68. https://doi.org/10.1007/s002110050253.
[178] Bendsøe MP, Kikuchi N. Generating optimal topologies in structural design using a homogenization method. Comput Method Appl Mech Eng 1988;71:197–224. https://doi.org/10.1016/0045-7825(88)90086-2.
[179] Cherkaev A. Variational methods for structural optimization. V. 140. Springer Science & Business Media; 2000.
[180] Almeida CJ, Cardoso JO, Coelho PG, Velhinho A, Xavier J, Borges JP. Architectured and additively manufactured double-negative index metamaterials. World Congr Comput Mech ECCOMAS Congr 2022:1–11. https://doi.org/10.23967/eccomas.2022.056.
[181] Almeida CJ, Conde FM, Coelho PG, Pratas TL. Stiffness and strength-based lightweight design of truss structures using multi-material topology optimization. In: 9th Int Conf Comput Methods Coupled Probl Sci Eng COUPLED Probl 2021; 2021. https://doi.org/10.23967/coupled.2021.052.
[182] Bendsoe, Martin Philip and OS. Topology optimization: theory, methods, and applications. Springer Science & Business Media; 2003.
[183] Paulino GH, Silva ECN. Design of functionally graded structures using topology optimization. Mater Sci Forum 2005;492–493:435–40. https://doi.org/10.4028/www.scientific.net/MSF.492-493.435.
[184] Brenner R. Computational approach for composite materials with coupled constitutive laws. Zeitschrift Für Angew Math Und Phys 2010;61:919–27. https://doi.org/10.1007/s00033-009-0045-8.
[185] Moulinec H, Suquet P. A numerical method for computing the overall response of nonlinear composites with complex microstructure. Comput Methods Appl Mech Eng 1998;157:69–94. https://doi.org/10.1016/S0045-7825(97)00218-1.
[186] Brenner R, Bravo-Castillero J. Response of multiferroic composites inferred from a fast-Fourier-transform-based numerical scheme. Smart Mater Struct 2010;19:115004. https://doi.org/10.1088/0964-1726/19/11/115004.
[187] Brenner R. Numerical computation of the response of piezoelectric composites using Fourier transform. Phys Rev B 2009;79:184106. https://doi.org/10.1103/PhysRevB.79.184106.
[188] Cavalcante MAA, Pindera M-J, Khatam H. Finite-volume micromechanics of periodic materials: past, present and future. Compos Part B Eng 2012;43:2521–43. https://doi.org/10.1016/j.compositesb.2012.02.006.
[189] Chen Q, Meraghni F, Chatzigeorgiou G. Recursive multiscale homogenization of multiphysics behavior of fuzzy fiber composites reinforced by hollow carbon nanotubes. J Intell Mater Syst Struct 2023;34:461–75. https://doi.org/10.1177/1045389X221111545.
[190] Pettermann HE, Suresh S. A comprehensive unit cell model: a study of coupled effects in piezoelectric 1–3 composites. Int J Solid Struct 2000;37:5447–64. https://doi.org/10.1016/S0020-7683(99)00224-3.
[191] Kar-Gupta R, Venkatesh TA. Electromechanical response of 1–3 piezoelectric composites: a numerical model to assess the effects of fiber distribution. Acta Mater 2007;55:1275–92. https://doi.org/10.1016/j.actamat.2006.09.042.
[192] Challagulla KS, Venkatesh TA. Electromechanical response of piezoelectric foams. Acta Mater 2012;60:2111–27. https://doi.org/10.1016/j.actamat.2011.12.036.
[193] Zhang X, Guo Y, Zhu F, Chen X, Tian H, Xu H. A linear-arc composite beam piezoelectric energy harvester modeling and finite element analysis. Micromachines (Basel) 2022;13:848. https://doi.org/10.3390/mi13060848.
[194] Chanda AG, Sahoo R. Finite element analysis of smart composite plate structures coupled with piezoelectric materials: investigation of static and vibration responses. Mech Adv Mater Struct 2022;29:6118–43. https://doi.org/10.1080/15376494.2021.1972372.